On nonlinear thermo-electro-elasticity

Markus Mehnert[a], Mokarram Hossain[a,b], Paul Steinmann[a,*]

[a] *Chair of Applied Mechanics, University of Erlangen-Nuremberg, Paul-Gordan Strasse 3, 91052 Erlangen, Germany*
[b] *Mechanical and Construction Engineering, Northumbria University, Newcastle upon Tyne, United Kingdom*

Abstract

Electro-active polymers (EAPs) for the case of large actuations are nowadays well-known and promising candidates in producing sensors, actuators and generators. In general, polymeric materials are sensitive to differential temperature histories. During experimental characterisations of EAPs under electro-mechanically coupled loads, it is difficult to maintain constant temperature not only due to an external differential temperature history but also thanks to the changes of internal temperature by the application of high electric loads. In this contribution, a thermo-electro-mechanically coupled constitutive framework is proposed based on the total energy approach. Departing from relevant laws of thermodynamics, thermodynamically consistent constitutive equations are formulated. To demonstrate the performance of the proposed thermo-electro-mechanically coupled framework, a frequently used non-homogeneous boundary value problem, i.e. the extension and inflation of a cylindrical tube is solved analytically. The results illustrate the influence of various thermo-electro-mechanical couplings.

Keywords: Electro-mechanical problem, Thermo-mechanical problem, Non-linear elasticity, Electro-active polymers, Thermo-electro-mechanical coupling

1. Introduction

In the last couple of decades, the so-called electro-active polymers (EAPs) have been gaining popularity within the smart materials community. The core mechanism of EAPs is an electro-mechanical coupling behavior that converts the energy of an electric field into mechanical energy. In contrast to traditional piezoelectric materials of small strain actuation mechanisms, the excitation on EAPs by an external electric field results in a large deformation. It may also result in a change in their material behavior, e.g. the polarization response. EAPs can be divided into two major categories depending on the mechanism of deformation: electronic electro-active polymers (EEAPs) and ionic electro-active polymers (IEAPs). In general, two electro-mechanical forces are mainly responsible for the deformation of the polymer. Firstly, the Maxwell stress that originates due to elastostatic forces between electric charges. Secondly, the electrostriction that is due to intramolecular forces of the material. Electro-active polymeric materials have potential applications, e.g. as dielectric elastomers (DEs) in artificial muscles, sensors and generators [6, 9, 10] . EEAP as a dielectric elastomer is utilized in the form of a thin film that is coated with two compliant electrodes and sandwiched in between them. The dielectric elastomer's thickness has to be thin-filmed for a large activation

*Corresponding author. Tel.: +49 09131-8528501; Fax: +49 09131-8528503.
Email addresses: markus.mehnert@ltm.uni-erlangen.de (Markus Mehnert), mokarram.hossain@northumbria.ac.uk (Mokarram Hossain), paul.steinmann@ltm.uni-erlangen.de (Paul Steinmann)

output with a moderate electric potential difference. When the thin-film is squeezed in the direction of the applied electric field, the material expands in the transverse planar direction as the underlying polymeric material is idealized as nearly incompressible material [15, 16, 17, 39, 40].

Experimental works of EAPs either under purely mechanical or electro-mechanical loading are very rare in the literature [31, 35]. Diaconu and co-workers [31] studied the electro-mechanical properties of a synthesized polyurethane (PU) elastomer film-based polyester. Therein, it has been verified that the deformation of a polyurethane elastomer varies quadratically due to the applied electric field. Qiang et al. [35] presented an experimental study on the dielectric properties of a polyacrylate dielectric elastomer. Ma and Cross [33] conducted an experimental investigation of the electromechanical response in a dielectric acrylic elastomer in various frequency ranges at room temperature. Michel et al. [34] performed a comparison between silicone and acrylic elastomers that can potentially be used as dielectric materials in electro-active polymer actuators. Moreover, natural rubber and styrene-based elastomers have recently demonstrated very good electro-mechanical properties (even better than silicone and acrylic elastomers) for the development of dielectric elastomer transducers, see for example, Vertechy et al., [7], Kaltseis et al. [8] .

Hossain et al. [63] at first did a comprehensive mechanical characterization of an acrylic elastomer (VHB 4910 by 3M) using different standard experiments such as single-step relaxation tests, multi-step relaxation tests, and loading-unloading cyclic tests. In modelling the mechanical behavior, a modified version of the micro-mechanically motivated Bergstroem-Boyce viscoelastic model [23, 24] has been used along with a finite linear evolution law. Later on, experiments with electro-mechanically coupled loads were conducted in Hossain el al. [64] considering standard tests already used for a viscoelastic polymeric material characterization in the purely mechanical case. In all experimental cases, the polymer samples were pre-stretched up to several hundred percent to achieve an initial thickness reduction in order to increase the effect of the applied electro-mechanically coupled load. Subsequently the pre-stretched samples were subjected to various amounts of mechanical as well as coupled deformations at different strain rates. The data produced from several loading-unloading tests, single-step relaxation tests, and multi-step relaxation tests show that the electric loading has profound effect in the time-dependent behavior of the VHB 4910 elastomer.

Recently Ask and co-workers [20, 21] modelled the electrostrictive behavior of viscoelastic polymers, particularly electrostrictive polyurethane (PU) elastomer, using a phenomenologically-motivated constitutive model. After proposing a thermodynamically consistent electro-mechanical coupled finite strain viscoelastic model based on a multiplicative decomposition of the deformation gradient, they used Johlitz et al. [28] data for identifying the purely mechanical parameters of the model and Diaconu et al. [31] data for the identification of the coupled parameters as well as for their model validation. Büschel and co-workers [22] proposed an electro-viscoelastic model using a multiplicative decomposition of the deformation gradient into an elastic part and a viscous part for the mechanical deformation where the mechanical free energy basically stems from an Ogden-type energy function [29]. Another interesting electro-viscoelastically coupled model is proposed by Vogel and co-workers [1, 2] . Following the classical approach of the deformation gradient decomposition, Saxena et al. [25, 26] proposed an electro-viscoelastic model that considers an additive decomposition of the vector-valued electric field variable into an equilibrium part and a non-equilibrium part. Compared to Vogel et al., Saxena and co-workers formulate their governing equations following the idea of McMeeking and Landis [32]. However, none of the earlier constitutive model takes a thermo-electro-mechanically coupled approach into account.

Vertechy and co-workers [4, 5] presented a finite-deformation thermo-electro-elastically coupled continuum model for electrostrictive elastomers. In the framework, they assumed EAPs as an isotropic modified-entropic hyperelastic dielectric that can deform under combined actions of electrical, thermal and mechanical stimuli. They have demonstrated the thermodynamical consistency of the formulation. Moreover, the formulation does not require the postulation of any force or stress tensor of electrical origin, cf. Vertechy [4]. In order to identify material parameters appearing in the model, they conducted a thermo-electro-elastically experimental study on a Lozenge-shaped linear actuator which is optimally designed for dielectric elastomers (DEs), cf. Vertechy et al. [5]. They were able to demonstrate an excellent correlation of the proposed thermo-electro-elastic model with the experimental data. However, the model is applied to the study of a uniaxial mechanical load case and the temperature distribution is assumed homogeneously for the selected geometry. Therefore, the solution of any real thermo-electro-mechanical boundary value problem is absent here.

A coupled theory for damage and time-dependence, e.g. viscoelasticity or aging of nonlinear thermo-electro-mechanical and thermo-magneto-mechanical problems is developed in Chen [56, 57]. Therein, the total energy includes the contribution of the electric field as a functional of the histories of stress, temperature, temperature gradient and electric field while an internal state variable is introduced in the case of damage modelling. The framework is developed in a thermodynamically consistent way. A superposition principle of time, aging, temperature, stress and electric field is proposed for materials with memory on an intrinsic time scale so that the long-term property functions may be represented with horizontal and vertical shifting of the momentary master curves. However, none of the purely theoretical contributions demonstrate solutions of any boundary value problem neither for thermo-electro-viscoelasticity nor for thermo-magneto-viscoelasticity.

In this contribution, we present a general constitutive framework for a thermo-electro-mechanical case departing from the second of law of thermodynamics and neglecting any time-dependent phenomenon. Starting with the standard definition of the heat capacity, we come up with a generalised formulation for the thermo-electro-mechanical free energy function in an additive form where the electro-mechanically coupled effect is linearly scaled with the temperature. Moreover, three different forms of electro-mechanical coupled energy functions are proposed. For the numerical case study, we analytically solve the extension and inflation of a cylindrical tube that works under a thermo-electro-mechanical load where, in addition to electro-mechanical loads, heat flow also occurs. To the best of the authors knowledge, this widely used benchmark problem is not solved yet in the literature for the thermo-electro-mechanically case. Polymeric materials are typically viscoelastic and non-perfect electrical insulators where temperature changes can also occur due to dissipation. In addition, there are various other sources for temperature changes, e.g. external heat flux or prescribed temperature boundary conditions. The current contribution proposes a general framework for electro-thermo-mechanical coupling whereby, however, temperature changes due to viscoelastic dissipation and current leakage are skipped for the sake of simplicity. Consideration of all sources of dissipations and the resulting temperature variations are important and will be addressed in our forthcoming contributions.

The paper is organized as follows: Section (2) will briefly review the non-linear kinematics and will elaborate basic equations in non-linear electro-mechanics. In Section (3), the main mathematical foundation that leads to a thermo-electro-mechanical formulation for electro-active polymers is discussed in detail. It includes coupled constitutive equations, the total energy function and the modified heat equation of the thermo-electro-mechanically coupled problem. A non-homogeneous boundary problem is solved analyti-

cally with the proposed formulation which is elaborated in Section (4). The final Section (5) concludes the paper with a summary and an outlook for future works.

2. Basics of non-linear electro-mechanics

2.1. Kinematics

In the case of large deformations we distinguish between the reference configuration $\mathcal{B}_0$ and the deformed configuration $\mathcal{B}_t$. We consider the body $\mathcal{B}$ as a composition of a set of particles. The placement of these particles in the reference configuration $\mathcal{B}_0$ is specified by the position vector $\boldsymbol{X}$. In the deformed configuration $\mathcal{B}_t$ the particle positions are described by the position vector $\boldsymbol{x}$ which is connected to $\boldsymbol{X}$ through the nonlinear deformation map $\boldsymbol{x} = \boldsymbol{\chi}(\boldsymbol{X})$. The deformation gradient $\boldsymbol{F}$ is defined as the gradient of the deformation map with respect to the material coordinates

$$\boldsymbol{F} = \text{Grad}\, \boldsymbol{\chi}; \quad J = \det \boldsymbol{F}, \tag{1}$$

where J is the Jacobian determinant of the deformation gradient. Using the deformation gradient we can introduce the left and right Cauchy-Green tensors $\boldsymbol{b}$ and $\boldsymbol{C}$, respectively,

$$\boldsymbol{b} = \boldsymbol{F}\boldsymbol{F}^T, \quad \boldsymbol{C} = \boldsymbol{F}^T\boldsymbol{F}. \tag{2}$$

2.2. Balance laws in electrostatics

2.2.1. Spatial configuration

The electric displacement $\mathbb{d}^{\varepsilon}$ in vacuum is coupled with the electric field $\mathbb{e}$ by the electric permittivity of vacuum ε_0

$$\mathbb{d}^{\varepsilon} = \varepsilon_0 \mathbb{e}, \quad \text{in } \mathcal{B}_t. \tag{3}$$

For condensed matter this equation is extended by the electric polarization $\mathbb{p}$ and is typically nonlinear in the electric field

$$\mathbb{d} = \varepsilon_0 \mathbb{e} + \mathbb{p} =: \mathbb{d}^{\varepsilon} + \mathbb{p}, \quad \text{in } \mathcal{B}_t. \tag{4}$$

For insulating materials without free current and free electric charges the electrical problem can be characterized by the Maxwell equations, for the quasi-static case

$$\text{curl}\, \mathbb{e} = \boldsymbol{0}, \quad \text{div}\, \mathbb{d} = 0 \quad \text{in } \mathcal{B}_t. \tag{5}$$

Equation $(5)_1$ is satisfied exactly by an electric field that is derived from a scalar potential [1, 14, 13, 30]. Therefore $\mathbb{e}$ is defined by

$$\mathbb{e} = -\text{grad}\, \varphi, \tag{6}$$

where grad φ is the gradient of the electric potential with respect to the spatial coordinates. The mechanical material behavior is governed by the balance of linear momentum

$$\text{div}\, \boldsymbol{\sigma} + \boldsymbol{b}_t^{\text{pon}} + \boldsymbol{b}_t = \text{div}\, \boldsymbol{\sigma}^{\text{tot}} + \boldsymbol{b}_t = \boldsymbol{0}, \quad \text{in } \mathcal{B}_t, \tag{7}$$

with the mechanical body force $\boldsymbol{b}_t$ and the total Cauchy type symmetric stress tensor $\boldsymbol{\sigma}^{\text{tot}}$ [39] that consists of a non-symmetric mechanical Cauchy stress $\boldsymbol{\sigma}$ and the ponderomotive stress $\boldsymbol{\sigma}^{\text{pon}}$ [17]

$$\text{div}\, \boldsymbol{\sigma}^{\text{pon}} = \boldsymbol{b}_t^{\text{pon}} = \text{grad}\, \mathbb{e} \cdot \mathbb{p}. \tag{8}$$

The ponderomotive stress can be decomposed into a non-symmetric polarization stress $\boldsymbol{\sigma}^{\text{pol}}$ [2, 3] and the symmetric Maxwell stress $\boldsymbol{\sigma}^{\text{max}}$

$$\boldsymbol{\sigma}^{\text{pol}} = \mathbb{e} \otimes \mathbb{p}, \quad \boldsymbol{\sigma}^{\text{max}} = -\frac{1}{2}\varepsilon_0[\mathbb{e} \cdot \mathbb{e}]\boldsymbol{i} + \varepsilon_0 \mathbb{e} \otimes \mathbb{e}, \tag{9}$$

where $\boldsymbol{i}$ is the second order identity tensor in the spatial configuration. Outside of matter the polarization $\mathbb{p}$, the Cauchy stress $\boldsymbol{\sigma}$ and the polarization stress $\boldsymbol{\sigma}^{\text{pol}}$ vanish but the Maxwell stress and the electric displacement $\mathbb{d}^{\epsilon}$ exist and satisfy a divergence free condition

$$\text{div}\, \boldsymbol{\sigma}^{\text{max}} = \mathbf{0}. \tag{10}$$

Along the boundary $\partial\mathcal{B}_t$ Dirichlet boundary conditions for the deformation map $\boldsymbol{\chi}$ are prescribed

$$\boldsymbol{\chi} = \boldsymbol{\chi}^{\text{p}}, \quad \text{on } \partial\mathcal{B}_t. \tag{11}$$

With the prescribed mechanical tractions $\boldsymbol{t}_t^{\text{p}}$ and the surface normal $\boldsymbol{n}$ on the surface of $\mathcal{B}_t$ the jump conditions can be defined as in [3]

$$[\![\boldsymbol{\sigma}^{\text{tot}}]\!] \cdot \boldsymbol{n} = -\boldsymbol{t}_t^{\text{p}}, \quad \text{on } \partial\mathcal{B}_t^{\text{t}}, \tag{12}$$

where $[\![\bullet]\!]$ represents the difference $[\bullet^{\text{out}} - \bullet^{\text{in}}]$. The jump conditions for the electrical quantities are defined as

$$[\![\mathbb{d}]\!] \cdot \boldsymbol{n} = \hat{\varrho}_t^f, \quad \text{on } \partial\mathcal{B}_t^{\varrho}, \quad \text{and} \quad [\![\mathbb{e}]\!] \times \boldsymbol{n} = 0, \quad \text{on } \partial\mathcal{B}_t \tag{13}$$

where $\hat{\varrho}_t^f$ is the density of free surface charges per undeformed area on the boundary [2]. These boundary conditions in combination with Eqn (6) lead to a continuity boundary condition

$$[\![\varphi]\!] = 0, \quad \text{on } \partial\mathcal{B}_t^{\varrho}, \tag{14}$$

and a Dirichlet boundary condition for the electric scalar potential where we can prescribe a value for the electric scalar potential

$$\varphi = \varphi^{\text{p}}, \quad \text{on } \mathcal{B}_t^{\varphi}. \tag{15}$$

2.2.2. Material configuration

Various electric quantities described in the previous section are expressed in the spatial configuration. We now want to transform them in the undeformed configuration $\mathcal{B}_0$ as

$$\mathbb{E} = \boldsymbol{F}^T \mathbb{e}, \quad \mathbb{D} = J\boldsymbol{F}^{-1}\mathbb{d}, \quad \mathbb{P} = J\boldsymbol{F}^{-1}\mathbb{p}, \tag{16}$$

so that the Maxwell equations are defined as

$$\text{Curl}\, \mathbb{E} = \mathbf{0}, \quad \text{Div}\, \mathbb{D} = 0, \tag{17}$$

where Curl and Div denote the corresponding differential operators with respect to the position vectors $\boldsymbol{X}$ in $\mathcal{B}_0$. The first term implies the existence of a scalar potential such that

$$\mathbb{E} = -\text{Grad}\, \varphi, \quad \text{in } \mathcal{B}_0. \tag{18}$$

We introduce a formulation for the electric displacement in the bulk as

$$\mathbb{D} = \varepsilon_0 J \boldsymbol{C}^{-1}\mathbb{E} + \mathbb{P} \quad \text{in } \mathcal{B}_0. \tag{19}$$

This referential format of the polarization follows unambiguously from a pull-back of the spatial format (4). However, this definition is not unique as, for example, the definition of the polarization might alter, c.f. [39]. The total Cauchy stress $\boldsymbol{\sigma}^{\text{tot}}$ can be transformed into a material counterpart, the total Piola stress tensor $\boldsymbol{P}^{\text{tot}}$

$$\boldsymbol{P}^{\text{tot}} = J\boldsymbol{\sigma}^{\text{tot}}\boldsymbol{F}^{-T}, \tag{20}$$

which can be decomposed into the mechanical part $\boldsymbol{P}$ and the ponderomotive part $\boldsymbol{P}^{\text{pon}}$

$$\boldsymbol{P}^{\text{tot}} = \boldsymbol{P} + \boldsymbol{P}^{\text{pon}} = \boldsymbol{P} + \boldsymbol{P}^{\text{max}} + \boldsymbol{P}^{\text{pol}}, \tag{21}$$

with the polarization stress $\boldsymbol{P}^{\text{pol}}$ and the Maxwell stress $\boldsymbol{P}^{\text{max}}$

$$\boldsymbol{P}^{\text{pol}} = \mathbb{e} \otimes \mathbb{P}, \ \boldsymbol{P}^{\text{max}} = -\left[\frac{1}{2}\varepsilon_0 J\mathbb{E}\cdot[\boldsymbol{C}^{-1}\mathbb{E}]\right]\boldsymbol{F}^{-T} + \mathbb{e}\otimes\mathbb{D}^{\varepsilon}, \tag{22}$$

whereby $\frac{1}{2}\varepsilon_0 J\mathbb{E}\cdot[\boldsymbol{C}^{-1}\mathbb{E}]$ denotes the electrostatic energy density per unit volume in the material configuration. The balance of linear momentum (7) and the divergence free condition of the Maxwell stress (10) are transformed to

$$\text{Div}\,\boldsymbol{P}^{\text{tot}} + \boldsymbol{b}_0 = \boldsymbol{0} \quad \text{and} \quad \text{Div}\,\boldsymbol{P}^{\text{max}} = \boldsymbol{0}. \tag{23}$$

The boundary conditions are translated to the material configuration such that

$$\begin{aligned} [\![\mathbb{D}]\!]\cdot\boldsymbol{N} &= \varrho_0^f, \quad \text{on } \partial\mathcal{B}_0^{\varrho}, \\ [\![\boldsymbol{P}^{\text{tot}}]\!]\cdot\boldsymbol{N} &= -\boldsymbol{t}_0^p, \quad \text{on } \partial\mathcal{B}_0^{t}, \end{aligned} \tag{24}$$

where conversions $\hat{\varrho}_0^f dA = \hat{\varrho}_t^f da$ and $\boldsymbol{t}_0^p dA = \boldsymbol{t}_t^p da$ are used to transfer these quantities from the material configuration with the area element dA to the spatial configuration with the respective area element da.

3. Basics of non-linear thermo-electro-mechanics

3.1. Constitutive equations

The energy density Ψ per unit volume in $\mathcal{B}_0$ is introduced as

$$\Psi = \tilde{\Psi}(\boldsymbol{F}, \theta, \mathbb{E}) \tag{25}$$

where θ is the absolute temperature. The second law of thermodynamics in the form of the Clausius-Duhem inequality leads to [27, 48]

$$\delta_0 = \left[\boldsymbol{P} + \boldsymbol{P}^{\text{pol}}\right] : \dot{\boldsymbol{F}} - \mathbb{P}\cdot\dot{\mathbb{E}} - \dot{\Psi} - H\dot{\theta} - \boldsymbol{Q}\cdot\frac{\text{Grad}(\theta)}{\theta} \geq 0, \tag{26}$$

where H is the entropy and $\boldsymbol{Q}$ is a heat flux vector defined in the material configuration that can be transformed to the spatial form via $J\boldsymbol{q} = \boldsymbol{F}\boldsymbol{Q}$. Taking the time derivative of $\Psi(\boldsymbol{F}, \theta, \mathbb{E})$ and inserting into Eqn

(26), the following constitutive relation can be obtained

$$\boldsymbol{P} + \boldsymbol{P}^{\text{pol}} = \frac{\partial \Psi}{\partial \boldsymbol{F}}, \quad \mathbb{P} = -\frac{\partial \Psi}{\partial \mathbb{E}}, \quad H = -\frac{\partial \Psi}{\partial \theta}. \tag{27}$$

As demonstrated by Dorfmann and Ogden [39, 40], it is useful to introduce a total energy density Ω according to

$$\Omega(\boldsymbol{F}, \theta, \mathbb{E}) = \Psi(\boldsymbol{F}, \theta, \mathbb{E}) + E(\boldsymbol{F}, \mathbb{E}). \tag{28}$$

As is demonstrated in [1] this changes the dissipation inequality to

$$\delta_0^* = \boldsymbol{P}^{\text{tot}} : \dot{\boldsymbol{F}} - \mathbb{D} \cdot \dot{\mathbb{E}} - \dot{\Omega} - H\dot{\theta} - \boldsymbol{Q} \cdot \frac{\text{Grad}(\theta)}{\theta} \geq 0, \tag{29}$$

and the constitutive relations modify to

$$\boldsymbol{P}^{\text{tot}} = \frac{\partial \Omega}{\partial \boldsymbol{F}}, \quad \text{with} \quad \boldsymbol{P}^{\text{max}} = \frac{\partial E}{\partial \boldsymbol{F}}, \quad \mathbb{D} = -\frac{\partial \Omega}{\partial \mathbb{E}}, \quad H = -\frac{\partial \Omega}{\partial \theta}. \tag{30}$$

Sometimes, it is convenient to express the total stress in terms of the Cauchy stress, i.e.

$$\boldsymbol{\sigma}^{\text{tot}} = J^{-1} \frac{\partial \Omega}{\partial \boldsymbol{F}} \boldsymbol{F}^T, \tag{31}$$

which in the case of incompressible materials is re-expressed as

$$\boldsymbol{\sigma}^{\text{tot}} = \frac{\partial \Omega}{\partial \boldsymbol{F}} \boldsymbol{F}^T - p\boldsymbol{i}, \tag{32}$$

where p is a Lagrange multiplier associated with the incompressibility constraint [16] and $\boldsymbol{i}$ is the second order identity tensor in the current configuration. After applying the Coleman-Noll argumentation [27] to Eqn (29), the reduced conductive dissipation power density reads

$$\delta_0^{\text{con}} = -\boldsymbol{Q} \cdot \frac{\text{Grad}(\theta)}{\theta} \geq 0. \tag{33}$$

3.2. Energy function

To derive a thermo-electro-mechanically coupled free energy function, we start with the heat capacity $c_{\boldsymbol{F},\mathbb{E}}$ at constant deformation and constant electric field, which is defined via the derivative of the energy with respect to the absolute temperature and likewise via the derivative of the entropy with respect to the absolute temperature [11, 12, 4, 55]. For the sake of simplicity and as an example, a constant heat capacity is assumed, whereby θ_0 is the reference temperature

$$c_{\boldsymbol{F},\mathbb{E}}(\theta) = c_{\boldsymbol{F},\mathbb{E}}(\theta_0) = c_0. \tag{34}$$

The heat capacity c_0 is also related to the negative second derivative of the energy Ψ with respect to the absolute temperature θ as

$$c_0 \quad = \quad -\theta \frac{\partial^2 \Psi}{\partial \theta \partial \theta} \stackrel{!}{=} \text{const.}, \quad \text{with} \quad \Psi = \Psi(\boldsymbol{F}, \theta, \mathbb{E}), \Rightarrow -\frac{c_0}{\theta} = \frac{\partial^2 \Psi}{\partial \theta \partial \theta}. \tag{35}$$

Integration from the reference temperature θ_0 to an arbitrary temperature θ leads to

$$\frac{\partial \Psi}{\partial \theta} = -c_0 \Big[\ln(\theta) - \ln(\theta_0) \Big] - C_1. \tag{36}$$

The integration constant C_1 may depend on the deformation gradient $\boldsymbol{F}$ and the electric field $\mathbb{E}$, i.e.

$$\frac{\partial \Psi}{\partial \theta} = -c_0 \ln\Big(\frac{\theta}{\theta_0}\Big) - C_1(\boldsymbol{F}, \mathbb{E}). \tag{37}$$

Integrating a second time from the reference temperature θ_0 to an arbitrary temperature θ brings us to

$$\Psi = \underbrace{c_0 \Big[\theta - \theta_0 - \theta \ln\Big(\frac{\theta}{\theta_0}\Big) \Big]}_{\text{capacitive contribution}} - \underbrace{\Big[\theta - \theta_0\Big] C_1(\boldsymbol{F}, \mathbb{E})}_{\text{coupled contr.}} + \underbrace{W(\boldsymbol{F}, \mathbb{E})}_{\text{isoth. contr.}}, \tag{38}$$

where the first part of the energy function is termed as the capacitive contribution to the thermo-electro-mechanical framework due to a temperature change. For isotropy, the second integration constant W depends on the electro-mechanical coupled invariants, i.e. I_1 to I_6 as $W(\boldsymbol{F}, \mathbb{E}) = W(I_1, \cdots I_6)$. Thereby the electro-mechanical coupled invariants $(I_1, I_2, I_4, I_5, I_6)$ are defined as a combination of the right Cauchy-Green tensor $\boldsymbol{C}$ and the electric field $\mathbb{E}$ in the material configuration

$$\begin{aligned} &I_1 = \text{tr}(\boldsymbol{C}); && I_2 = \frac{1}{2}\Big[[\text{tr}(\boldsymbol{C})]^2 - \text{tr}(\boldsymbol{C}^2)\Big]; && I_3 = \det(\boldsymbol{F}); \\ &I_4 = [\mathbb{E} \otimes \mathbb{E}] : \boldsymbol{I}; && I_5 = [\mathbb{E} \otimes \mathbb{E}] : \boldsymbol{C}^{-1}; && I_6 = [\mathbb{E} \otimes \mathbb{E}] : \boldsymbol{C}^{-2}. \end{aligned} \tag{39}$$

The integration constant C_1 contains electro-mechanical contributions which we decompose additively into a purely mechanical part $M(\boldsymbol{F})$ and an electro-mechanically coupled part $C(\boldsymbol{F}, \mathbb{E})$, i.e.

$$C_1(\boldsymbol{F}, \mathbb{E}) = M(\boldsymbol{F}) + C(\boldsymbol{F}, \mathbb{E}). \tag{40}$$

The thermo-mechanical coupling effect leads to an increase in temperature for polymeric materials which is called the Gough-Joule effect, cf. [65]. Note that as a first step towards modelling thermo-electro-elasticity, the non-trivial problem of incompressibility in combination with thermal expansion is skipped here, for more discussions, see Leslie and Scott [66] . In the case of large strains, we here recall two possible forms of the mechanical part $M(\boldsymbol{F})$, i.e.

- $M(\boldsymbol{F}) = 3\kappa\alpha \ln(J)$
- $M(\boldsymbol{F}) = 3\kappa\alpha \frac{J^\gamma - 1}{\gamma}$

where α and κ are the thermal expansion and bulk modulus coefficients at the reference temperature and γ is a dimensionless constant material parameter. Note that since $M(\boldsymbol{F})$ only accounts for volumetric changes, it vanishes for incompressible materials. For the electro-mechanically coupled part $C(\boldsymbol{F}, \mathbb{E})$, we propose different possible combinations in the following.

If we do not consider any thermo-electro-mechanical coupling, the electro-mechanically coupled part simply vanishes, i.e.

- $C(\boldsymbol{F}, \mathbb{E}) = 0.$

When thermo-electro-mechanical coupling effects are considered with a pyroelectric coefficient π_0 and the deformation is neglected, the formulation reads

- $C(\boldsymbol{F}, \mathbb{E}) = -\frac{1}{2}\pi_0 \Big|\mathbb{E}\Big|^2 = -\frac{1}{2}\pi_0 \Big[[\mathbb{E} \otimes \mathbb{E}] : \boldsymbol{I}\Big] = -\frac{1}{2}\pi_0 I_4$

where I_4 is the fourth invariant defined in Eqn (39). In the third case thermo-electro-mechanical effects are considered, thus we assume

- $C(\boldsymbol{F}, \mathbb{E}) = -\frac{1}{2}\pi_0 J \mathbb{E}\boldsymbol{C}^{-1}\mathbb{E} = -\frac{1}{2}\pi_0 J \Big[\Big[\mathbb{E} \otimes \mathbb{E}\Big] : \boldsymbol{C}^{-1}\Big] = -\frac{1}{2}\pi_0 J I_5$

where I_5 is the fifth invariant defined in Eqn (39). This will give a pyroelectric stress in a form analogous to the Maxwell stress as

$$\boldsymbol{P}^{\text{pyro}} = \frac{\partial C(\boldsymbol{F}, \mathbb{E})}{\partial \boldsymbol{F}} = C(\boldsymbol{F}, \mathbb{E})\boldsymbol{F}^{-T} - \mathbb{e} \otimes J\pi_0 \boldsymbol{C}^{-1}\mathbb{E} \tag{41}$$

and the polarization is derived as

$$\mathbb{P} = -\frac{\partial \Psi}{\partial \mathbb{E}} = -\frac{\partial W(\boldsymbol{F}, \mathbb{E})}{\partial \mathbb{E}} + \Big[\theta - \theta_0\Big]\frac{\partial C(\boldsymbol{F}, \mathbb{E})}{\partial \mathbb{E}} = \mathbb{P}(\theta_0) + \Big[\theta - \theta_0\Big]\pi_0 J\boldsymbol{C}^{-1}\mathbb{E}. \tag{42}$$

This implies for the electric displacement in the bulk

$$\mathbb{D} = \varepsilon_0 J\boldsymbol{C}^{-1}\mathbb{E} + \mathbb{P} = \Big[\varepsilon_0 + \Big[\theta - \theta_0\Big]\pi_0\Big]J\boldsymbol{C}^{-1}\mathbb{E} + \mathbb{P}(\theta_0). \tag{43}$$

In the fourth case, we assume a relation which is consistent with the existing literature, cf. Vertechy et al. [4]. A formulation comparable to the one found in [4] can be obtained if we put

- $C(\boldsymbol{F}, \mathbb{E}) = -\frac{1}{\theta_0}W(\boldsymbol{F}, \mathbb{E}).$

The last relation will eventually yield a complete thermo-electro-mechanically coupled energy function as

$$\Psi(\boldsymbol{F}, \theta, \mathbb{E}) = \frac{\theta}{\theta_0}W(\boldsymbol{F}, \mathbb{E}) + c_0\Big[\theta - \theta_0 - \theta \ln\Big(\frac{\theta}{\theta_0}\Big)\Big] - \Big[\theta - \theta_0\Big]M(\boldsymbol{F}). \tag{44}$$

3.3. Heat equation

Considering the first law of thermodynamics, the governing equation used to describe the thermal field can be written in entropy form as

$$\theta\dot{H} = \mathcal{R} - \text{Div}\boldsymbol{Q}, \tag{45}$$

with the heat source $\mathcal{R}$ and the heat flux vector $\boldsymbol{Q}$ in the material configuration. By using the constitutive relation $H = -\frac{\partial \Psi}{\partial \theta}$ with the help of the chain rule and the definition of the specific heat capacity c_0, we obtain

$$\theta\dot{H} = -\theta\frac{\partial^2 \Psi}{\partial\theta\partial\theta}\dot{\theta} - \theta\frac{\partial^2 \Psi}{\partial \boldsymbol{F}\partial\theta} : \dot{\boldsymbol{F}} - \theta\frac{\partial^2 \Psi}{\partial \mathbb{E}\partial\theta} \cdot \dot{\mathbb{E}}. \tag{46}$$

Combining Eqns (45) and (46), the heat conduction equation is obtained as

$$c_0\dot{\theta} = \mathcal{R} - \mathrm{Div}\boldsymbol{Q} + \theta\partial_\theta\Big[\boldsymbol{P}^{\mathrm{tot}} : \dot{\boldsymbol{F}} - \mathbb{D}\cdot\dot{\mathbb{E}}\Big], \tag{47}$$

where the parts of the equation containing $\dot{\boldsymbol{F}}$ and $\dot{\mathbb{E}}$ correspond to the structural thermo-mechanical cooling/heating effect and the thermo-electric heating/cooling effect, respectively, see Vertechy et al. [4] for a similar expression.

4. Non-homogeneous boundary value problems

In this section, the above thermo-electro-mechanical framework is applied to a controllable non-homogeneous deformation, e.g. the extension and inflation of an incompressible cylindrical tube with a cylindrical symmetry, cf. [42, 43, 44, 45, 53]. Therefore, for the considered tube problem it is reasonable to work in cylindrical coordinates. Expressing the divergence of the electric displacement $\mathrm{div}\,\mathbb{d} = 0$ in cylindrical coordinates in the actual configuration, we find

$$\frac{1}{r}\mathbb{d}_r + \frac{\partial \mathbb{d}_r}{\partial r} + \frac{1}{r}\frac{\partial \mathbb{d}_\phi}{\partial \phi} + \frac{\partial \mathbb{d}_z}{\partial z} = 0, \tag{48}$$

and for the curl of the electric field $\mathrm{curl}\,\mathbb{e} = \boldsymbol{o}$

$$\frac{1}{r}\frac{\partial \mathbb{e}_z}{\partial \phi} - \frac{\partial \mathbb{e}_\phi}{\partial z} = 0; \quad \frac{\partial \mathbb{e}_r}{\partial z} - \frac{\partial \mathbb{e}_z}{\partial r} = 0; \quad \frac{1}{r}\frac{\partial (r\mathbb{e}_\phi)}{\partial r} - \frac{1}{r}\frac{\partial \mathbb{e}_r}{\partial \phi} = 0, \tag{49}$$

where $(\mathbb{e}_r, \mathbb{e}_\phi, \mathbb{e}_z)$ are the components of the electric field $\mathbb{e}$ and $(\mathbb{d}_r, \mathbb{d}_\phi, \mathbb{d}_z)$ are the components of the electric displacement $\mathbb{d}$. As we are only interested in cylindrically symmetric cases, so that $\frac{\partial(\bullet)}{\partial\phi} = \frac{\partial(\bullet)}{\partial z} = 0$, equations (48) and (49) reduce to

$$r\mathbb{d}_r = \text{constant}; \quad r\mathbb{e}_\phi = \text{constant}; \quad \mathbb{e}_z = \text{constant}. \tag{50}$$

The divergence of the stress tensor in cylindrical coordinates in a cylindrically symmetric stress state is expressed as

$$\mathrm{div}\,\boldsymbol{\sigma}^{\mathrm{tot}} = \left[\frac{\partial \sigma^{\mathrm{tot}}_{rr}}{\partial r} + \frac{\sigma^{\mathrm{tot}}_{rr} - \sigma^{\mathrm{tot}}_{\phi\phi}}{r}\right]\boldsymbol{e}_r + \left[\frac{\partial \sigma^{\mathrm{tot}}_{r\phi}}{\partial r} + \frac{2\sigma^{\mathrm{tot}}_{r\phi}}{r}\right]\boldsymbol{e}_\phi + \left[\frac{\partial \sigma^{\mathrm{tot}}_{rz}}{\partial r} + \frac{\sigma^{\mathrm{tot}}_{rz}}{r}\right]\boldsymbol{e}_z. \tag{51}$$

4.1. Extension and inflation of a tube

We consider a thick-walled tube in cylindrical coordinates, see Fig (1). The geometry in the spatial configuration is described by

$$a_i \le r \le a_e; \quad 0 \le \phi \le 2\pi; \quad 0 \le z \le l, \tag{52}$$

and in the material configuration by

$$A_i \le R \le A_e; \quad 0 \le \Phi \le 2\pi; \quad 0 \le Z \le L. \tag{53}$$

The electric field can generally have entries in radial and in z-direction ($\mathbb{e}_r = \lambda_r \mathbb{E}_R = \frac{1}{\lambda\lambda_r}\mathbb{E}_R$ and $\mathbb{e}_z =$

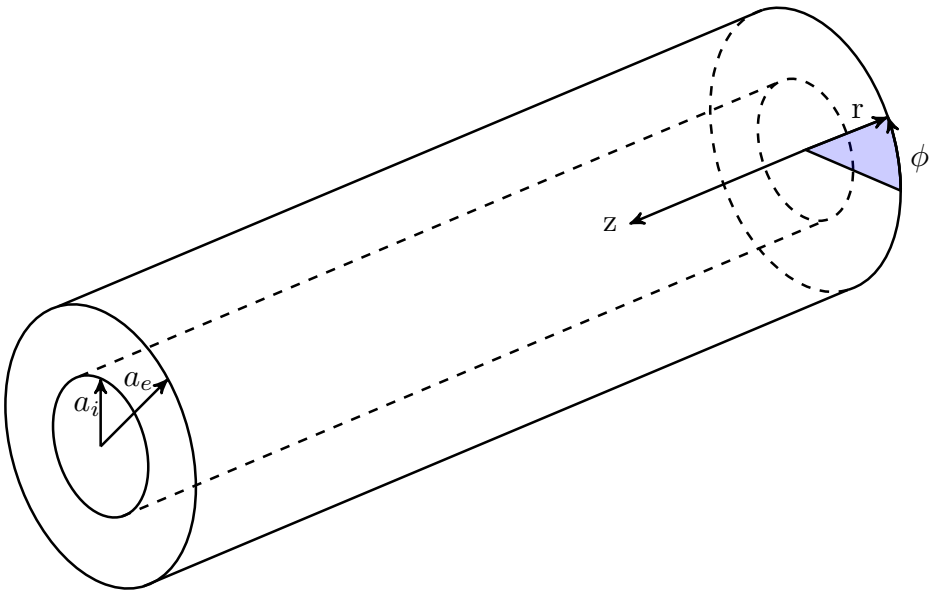

Figure 1: A thick-walled tube with inner diameter a_i and outer diameter a_e

$\lambda_z \mathbb{E}_Z$). An inflation with a simultaneous extension can be described by

$$r^2 = \lambda_z^{-1}\Big[R^2 - A_i^2\Big] + a_i^2, \quad \phi = \Phi, \quad z = \lambda_z Z, \tag{54}$$

where the main stretches in coordinate directions (r, Φ, z) are defined as

$$\lambda_r = [\lambda\lambda_z]^{-1}; \quad \lambda_\phi = \frac{r}{R} = \lambda; \quad \lambda_z. \tag{55}$$

For the inflation and extension of the tube, the divergence of the stress div$\boldsymbol{\sigma} = \boldsymbol{o}$ can be formulated from Eqn (51) as

$$\frac{\partial \sigma_{rr}^{\text{tot}}}{\partial r} + \frac{\sigma_{rr}^{\text{tot}} - \sigma_{\phi\phi}^{\text{tot}}}{r} = 0, \tag{56a}$$

$$\frac{\partial \sigma_{r\phi}^{\text{tot}}}{\partial r} + \frac{2\sigma_{r\phi}^{\text{tot}}}{r} = 0 \tag{56b}$$

$$\frac{\partial \sigma_{rz}^{\text{tot}}}{\partial r} + \frac{1}{r}\sigma_{rz}^{\text{tot}} = 0. \tag{56c}$$

With the constitutive relation (32), for incompressibility the total Cauchy stress can be calculated as

$$\begin{aligned}
\boldsymbol{\sigma}^{\text{tot}} &= \frac{\partial \Omega}{\partial \boldsymbol{F}} \boldsymbol{F}^T - p\boldsymbol{i} \\
&= \left[\frac{\partial \Omega}{\partial I_1}\frac{\partial I_1}{\partial \boldsymbol{F}} + \frac{\partial \Omega}{\partial I_2}\frac{\partial I_2}{\partial \boldsymbol{F}} + \frac{\partial \Omega}{\partial I_5}\frac{\partial I_5}{\partial \boldsymbol{F}} + \frac{\partial \Omega}{\partial I_6}\frac{\partial I_6}{\partial \boldsymbol{F}}\right] \boldsymbol{F}^T - p\boldsymbol{i} \\
&= 2\Omega_1 \boldsymbol{b} + 2\Omega_2[I_1\boldsymbol{b} - \boldsymbol{b}^2] - p\boldsymbol{i} - 2\Omega_5 \mathbb{e} \otimes \mathbb{e} - 2\Omega_6[\boldsymbol{b}^{-1}\mathbb{e} \otimes \mathbb{e} + \mathbb{e} \otimes \boldsymbol{b}^{-1}\mathbb{e}].
\end{aligned} \tag{57}$$

This leads to the non-zero stress components of $\boldsymbol{\sigma}^{\text{tot}}$

$$\begin{aligned}
\sigma_{rr}^{\text{tot}} &= -p + 2\lambda^{-2}\lambda_z^{-2}\Big[\Omega_1 + \Omega_2[\lambda^2 + \lambda_z^2]\Big] - 2[\Omega_5 + 2\Omega_6\lambda^2\lambda_z^2]\lambda^2\lambda_z^2\mathbb{E}_r^2,\\
\sigma_{\phi\phi}^{\text{tot}} &= -p + 2\lambda^2\Big[\Omega_1 + \Omega_2[\lambda^{-2}\lambda_z^{-2} + \lambda_z^2]\Big],\\
\sigma_{zz}^{\text{tot}} &= -p + 2\lambda_z^2\Big[\Omega_1 + \Omega_2[\lambda^{-2}\lambda_z^{-2} + \lambda^2]\Big] - 2[\Omega_5 + 2\Omega_6\lambda_z^{-2}]\lambda_z^{-2}\mathbb{E}_z^2,\\
\sigma_{rz}^{\text{tot}} &= -2\mathbb{E}_r\mathbb{E}_z\Big[\Omega_5 + \Omega_6[\lambda^2\lambda_z^2 + \lambda_z^{-2}]\Big].
\end{aligned} \tag{58}$$

4.1.1. Temperature function

In order to allow for an analytical solution available in the literature [18, 19], we neglect the thermo-mechanical and thermo-electrical cooling/heating effects. As a result, the heat equation from Eqn (47) simply yields

$$c_0\dot{\theta} = \mathcal{R} - \text{Div}\boldsymbol{Q}. \tag{59}$$

Considering steady-state conditions and neglecting any source terms $\mathcal{R}$, the equation can be written in the actual configuration as

$$\Delta_{\boldsymbol{x}}\theta = 0, \tag{60}$$

where $\boldsymbol{q} = -\kappa\text{grad}\theta$ and Δ is a Laplacian operator. In this case a constant value for the spatial thermal conductivity κ has been assumed. Note that the considered expression is a special case which, in the case of any dependency on both deformation and electric field, needs to be extended to incorporate more complex coupling effects by choosing a different constitutive equation. For more details we refer for example to the works of Eringen and Maugin [67]. In the (quasi) static case, the heat equation is reduced to the Laplace equation [18] which is also known as the stationary heat equation. In the cylindrical coordinates (r, ϕ, z) the equation for an axial symmetric problem, e.g. a cylindrical hollow tube can be written as

$$\frac{\mathrm{d}^2\theta(r)}{\mathrm{d}r^2} + \frac{1}{r}\frac{\mathrm{d}\theta(r)}{\mathrm{d}r} = 0, \tag{61}$$

where r is the actual radius of the tube. An analytical solution for the equation can be found in Bland et al. [18] and also in Rajagopoal and Huang [19]

$$\theta(r) = k_1 + k_2\ln r. \tag{62}$$

This indicates a logarithmically varying temperature profile along the radial thickness of the tube. Constants k_1 and k_2 can be determined by the boundary conditions at the inner and outer surfaces of the tube. For an internal radius a_i and an external radius a_e with the corresponding actual temperatures $\theta(a_i)$ and $\theta(a_e)$, respectively, we find

$$\begin{aligned}
k_1 &= \frac{\theta(a_i)\ln(a_e) - \theta(a_e)\ln a_i}{\ln a_e - \ln a_i},\\
k_2 &= \frac{\theta(a_e) - \theta(a_i)}{\ln a_e - \ln a_i}.
\end{aligned} \tag{63}$$

4.1.2. Axially applied electric field

Now, an energy function W at the reference temperature is required. As an example, we assume an incompressible Neo-Hookean-like material as in [13, 30] depending on the purely mechanical invariant I_1, the shear modulus μ that depends on the purely electrical invariant I_4, the coupled invariant I_5 and the constants

c_1, c_2. Other advanced forms of energy functions for rubber-like materials can be coupled with the electric part of the energy to improve the modelling, cf. [23, 36, 61, 62]. Without considering the surrounding free space, the energy function is formulated as

$$W = \frac{\mu(I_4)}{2}[I_1 - 3] + c_1 I_4 + c_2 I_5 \tag{64}$$

where the coupled invariants $(I_1, I_2, I_4, I_5, I_6)$ are defined in Eqn (39). Note that this type of free energy function incorporating electro-mechanical coupling is frequently used in the literature [1, 2, 15, 16, 63] and is motivated by Neo-Hookean type pure mechanical response modelling of rubber-like materials. It should be noted that the large deformations considered here lead to a strong polarization of the material. Due to the small value of the vacuum permittivity the free space term in the total energy formulation (28) can be neglected as in [13] and it holds that $\Omega(\boldsymbol{F}, \theta, \mathbb{E}) \approx \Psi(\boldsymbol{F}, \theta, \mathbb{E})$. As has been proposed in [15], we approximate the shear modulus with a linear function so that $\mu(I_4) = g_0 + g_1 I_4$, where g_0, g_1 are material parameters. Therefore, the derivatives $\frac{\partial \Omega_i}{\partial I_i} =: \Omega_i$ with respect to the invariants are

$$\Omega_1 = \frac{\theta}{2\theta_0}\left[g_0 + g_1 I_4\right], \quad \Omega_2 = \Omega_6 = 0, \quad \Omega_4 = \frac{\theta}{\theta_0} c_1, \quad \Omega_5 = \frac{\theta}{\theta_0} c_2. \tag{65}$$

For an electric field applied in the axial direction, various invariants defined in Eqn (39) reduce to

$$I_4 = \mathbb{E}_z^2 = E_0^2; \quad I_5 = \lambda_z^{-2} I_4; \quad I_6 = \lambda_z^{-4} I_4. \tag{66}$$

After rearranging Eqn (56a) we obtain

$$\sigma_{rr}^{\text{tot}}(\bar{r}) = \int_{a_i}^{\bar{r}} \frac{1}{r}\Big[\sigma_{\phi\phi}^{\text{tot}}(r) - \sigma_{rr}^{\text{tot}}(r)\Big]\,\mathrm{d}r + c, \tag{67}$$

where c is an integration constant which can be determined from the boundary conditions for the stress. If the outer surface of the tube is free of mechanical loads we find

$$\begin{aligned} c &= -\int_{a_i}^{a_e} \frac{1}{r}\Big[\sigma_{\phi\phi}^{\text{tot}}(r) - \sigma_{rr}^{\text{tot}}(r)\Big]\,\mathrm{d}r + \sigma_{rr}^{\text{max}}(a_e) \\ &= \int_{a_i}^{a_e} \frac{1}{r}\Big[\sigma_{rr}^{\text{tot}}(r) - \sigma_{\phi\phi}^{\text{tot}}(r)\Big]\,\mathrm{d}r + \sigma_{rr}^{\text{max}}(a_e). \end{aligned} \tag{68}$$

At the inner boundary, the tube is subjected to a uniform pressure P

$$\sigma_{rr}^{\text{tot}}(a_i) = \sigma_{rr}^{\text{max}}(a_i) - P, \tag{69}$$

that leads to

$$\begin{aligned} \sigma_{rr}^{\text{tot}}(a_i) &= \int_{a_i}^{a_i} \frac{1}{r}\Big[\sigma_{\phi\phi}^{\text{tot}}(r) - \sigma_{rr}^{\text{tot}}(r)\Big]\,\mathrm{d}r + c \\ &= \int_{a_i}^{a_e} \frac{1}{r}\Big[\sigma_{rr}^{\text{tot}}(r) - \sigma_{\phi\phi}^{\text{tot}}(r)\Big]\,\mathrm{d}r + \sigma_{rr}^{\text{max}}(a_e) = \sigma_{rr}^{\text{max}}(a_i) - P. \end{aligned} \tag{70}$$

Due to the axially applied electric field, the electric field lines will be ideally aligned parallel to the longitudinal axis of the tube and do not depend on the radius. Therefore, the influence of the field in the inner and

outer surfaces are almost the same, so that $\sigma_{rr}^{\max}(a_i) = \sigma_{rr}^{\max}(a_e)$. Therefore, we obtain

$$P = \int_{a_i}^{a_e} \frac{1}{r}\Big[\sigma_{\phi\phi}^{\text{tot}}(r) - \sigma_{rr}^{\text{tot}}(r)\Big]\mathrm{d}r. \tag{71}$$

Now we can use the stress definitions from Eqn (58) in combination with (65) to read

$$P = \frac{[g_0 + g_1 I_4]}{\theta_0} \int_{a_i}^{a_e} \Big[k_1 + k_2 \ln(r)\Big]\frac{1}{r}\Big[\lambda^2 - \lambda^{-2}\lambda_z^{-2}\Big]\mathrm{d}r. \tag{72}$$

The integral can be decomposed into two parts

$$\begin{aligned} P = &\underbrace{\frac{[g_0 + g_1 I_4]}{\theta_0} \int_{a_i}^{a_e} k_1 \frac{1}{r}\Big[\lambda^2 - \lambda^{-2}\lambda_z^{-2}\Big]\mathrm{d}r}_{P_1} \\ &+ \underbrace{\frac{[g_0 + g_1 I_4]}{\theta_0} \int_{a_i}^{a_e} k_2 \ln(r)\frac{1}{r}\Big[\lambda^2 - \lambda^{-2}\lambda_z^{-2}\Big]\mathrm{d}r}_{P_2}. \end{aligned} \tag{73}$$

The term k_1 from the temperature equation (63) does not depend on the actual radius r. Hence, as is demonstrated in the Appendix, the first part of the pressure P_1 can be expressed as

$$P_1 = \frac{[g_0 + g_1 I_4]k_1}{\theta_0 \lambda_z}\Big[\ln\left(\frac{\lambda_i}{\lambda_e}\right) - \frac{1}{2\lambda_z}\Big[\lambda_i^{-2} - \lambda_e^{-2}\Big]\Big], \tag{74}$$

where $\lambda_i = a_i/A_i, \quad \lambda_e = a_e/A_e$. The second integral contains an expression that is very difficult to calculate with analytical integration methods. Therefore, it is solved using the computing environment Maple 18 [54]. Detailed derivations are given in the Appendix.

Another important term for the demonstration of the results for this tube example is the normal force $\mathcal{N}$ that is applied at the end faces of the tube. It is the force that is required for an axial extension or compression and is given by

$$\mathcal{N} = 2\pi \int_{a_i}^{a_e} \sigma_{zz} r \mathrm{d}r = 2\pi \int_{a_i}^{a_e} \Big[\sigma_{zz}^{\text{tot}} - \sigma_{zz}^{\max}\Big] r \mathrm{d}r. \tag{75}$$

Here σ_{zz} denotes the axial component of the mechanical traction that is applied. With the stress definitions (58), the definition of the axial component of the Maxwell stress is $\sigma_{zz}^{\max} = \frac{1}{2}\varepsilon_0 \lambda_z^{-2} E_0^2$ [16] and the material parameter $c_2 = \varepsilon_0/2$. Each term of the integral on the right hand side of equation (75) is evaluated separately (see Appendix). In the isothermal case, the normal force can be expressed as

$$\mathcal{N} = A_i^2 \pi\Big[g_0 + g_1 E_0^2\Big]\Big[\Big[\lambda_z^4 - \frac{\lambda_z \lambda_e^2 + 1}{2\lambda_e^2}\Big]\Big[\lambda_e^2 \zeta^2 - \lambda_i^2\Big] + \ln\left(\frac{\lambda_i}{\lambda_e}\right)\Big] + \pi\varepsilon_0 E_0^2\Big[\lambda_z^4 - 1\Big]\Big[\lambda_e^2\zeta^2 - \lambda_i^2\Big] \tag{76}$$

which coincides with the results displayed in various Figures by Bustamante [15] for an equivalent magneto-active problem. The normal force is transformed into a scaled axial load $\bar{\mathcal{N}} = \frac{\mathcal{N}}{A_i^2 \pi}$. In Eqn (76), the dimensionless thickness parameter is $\zeta = A_e/A_i$. The introduction of a temperature gradient adds a number of terms to the formulation of the normal force and leads to an expression that is significantly larger than the equivalent expression for the pressure presented above. Therefore, the final expression is presented only in

the Appendix. The constants used in the subsequent calculations are summarized in Table 1. The values of g_0 and g_1 are taken from Bustamante [15].

Table 1: Various material constants used in the subsequent calculations.

g_0 [kPa]	g_1 [kPa/[kV/m]^2]	ε_0 [F/m]
10^2	-1.0×10^{-3}	8.85×10^{-12}

4.1.3. Results and discussions

In order to illustrate the general behavior of the example we initially focus on the electro-mechanical load case for a cylindrical tube with the initial internal radius of 10 mm. Thus we prescribe an axial stretch λ_z, a radial inflation or compression characterized by λ_i, the ratio of the internal radius after the deformation to the initial radius and a purely axial electric field. In Figure (2) the radial pressure P is plotted for selected values of the electric field $\mathbb{E}$ and ζ, i.e. the ratio of the initial external to the initial internal radii, depending on the parameters λ_i and λ_z without the influence of a temperature gradient.

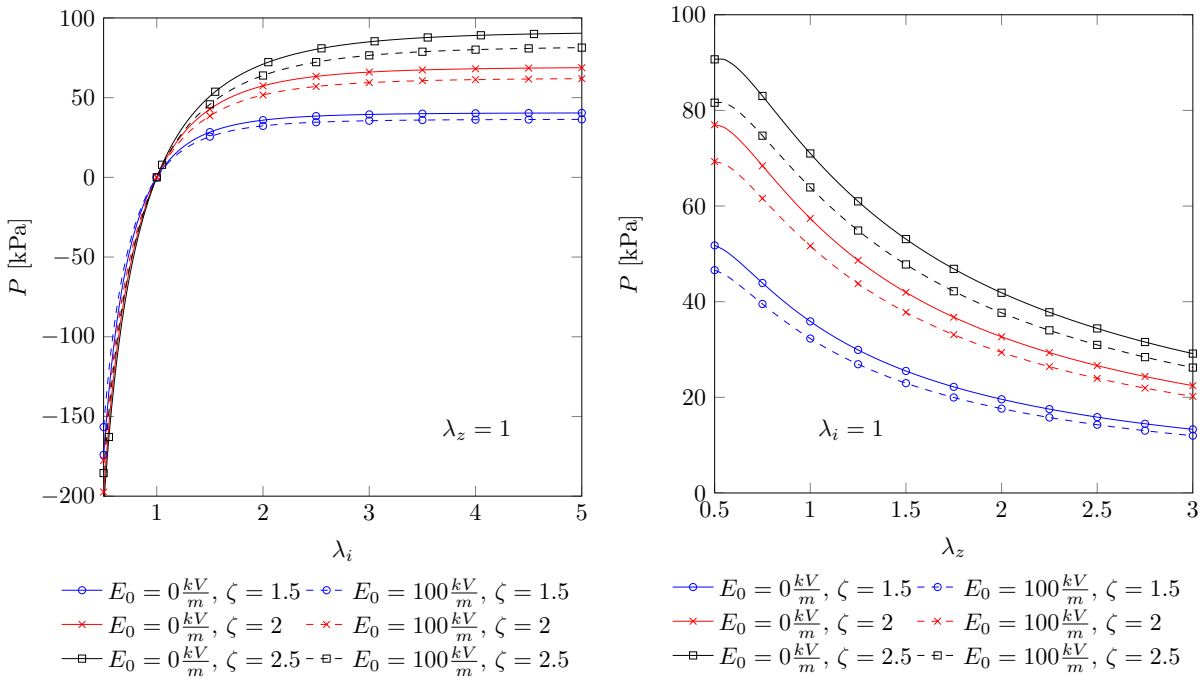

Figure 2: Plot of the pressure with respect to λ_i and λ_z under an electro-mechanically coupled load for various values of ζ

Fig (2a) shows that for the inflation of the tube ($\lambda_i > 1$), a positive pressure has to be applied on the internal surface. This pressure increases with increasing values of λ_i. In the case of a radial compression ($\lambda_i \leq 1$) we find that the pressure is negative which is decreasing for smaller values of λ_i. Furthermore it is visible in Fig (2a) that the material softens due to the applied electric field as the magnitude of the pressure decreases. In contrast to an axial compression $\lambda_z < 1$, the applied pressure at the inner surface is positive and it is reducing for increasing values of λ_z, cf. Fig (2b). An increase of the wall thickness of the tube

characterized by larger values of ζ leads to a higher pressure level that is needed both for the inflation or the axial stretch of the tube. In both plots of Fig (2), it is visible that the influence of the electric field on the applied pressure increases for larger values of ζ leading to a more distinctive reduction of the pressure.

Now we also incorporate a temperature gradient along the radial axis. To achieve this, the temperature at the outer surface of the tube θ_e is varied but the temperature at the internal surface is kept at the reference value θ_0. An increase of the absolute temperature θ_e ($\theta_e > \theta_0$) leads to a pressure increase. By cooling the external tube surface keeping the external temperature less than the reference one ($\theta_e < \theta_0$) the pressure decreases, cf. Fig (3). This behavior is typical for a rubber-like material in which the stresses increase with increasing temperature as presented for example in [68].

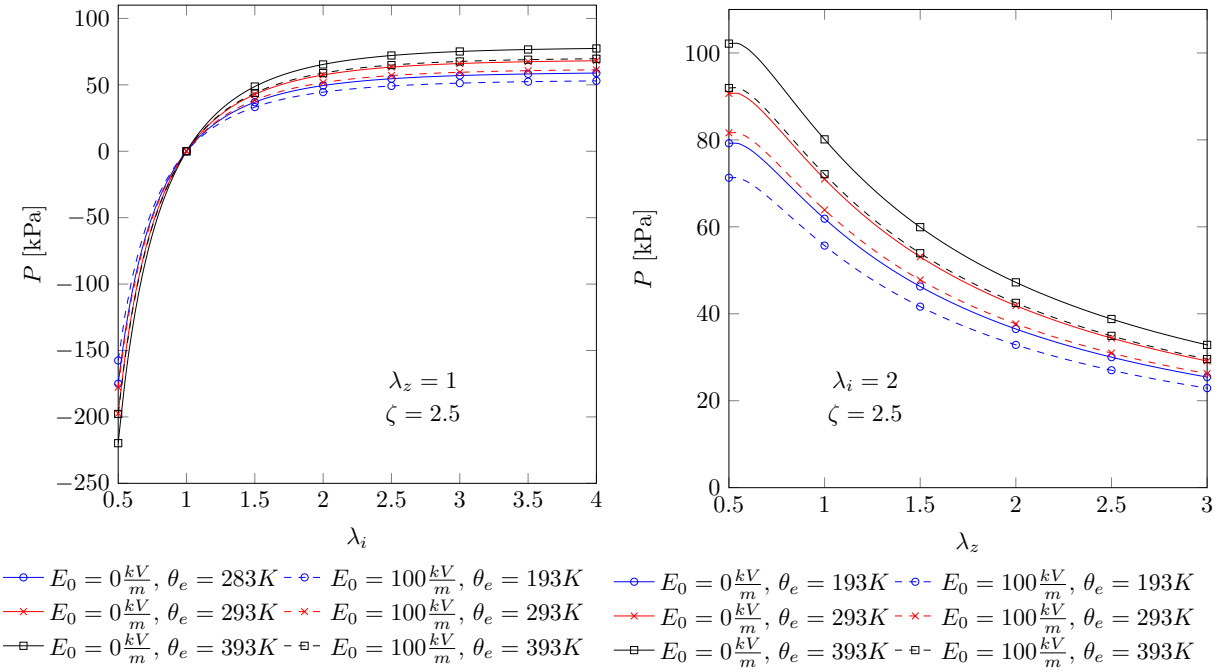

Figure 3: Plot of the pressure in the thermo-electro-mechanical case depending on λ_i, λ_z for selected values of ζ

Next we investigate the variation of the pressure with respect to the thickness ratio ζ and the electric field strength E_0 in the axial direction.

It is obvious that for a larger value of ζ, we find an increase in the magnitude of the pressure, cf. Fig (4). Furthermore, with a larger value of ζ the absolute difference between the pressure in the isothermal case and the cases with heating or cooling becomes larger but the ratio of the pressure in these two cases decreases. The latter shows a decreased influence of the temperature change due to the increased wall thickness. This is explained in more detail in the later examples.

We will now focus on the behavior of the scaled normal force $\bar{\mathcal{N}}$. As before, to illustrate the isothermal behavior of the system we start with a brief look at the electro-mechanical case, cf. Fig (5). As an inflation

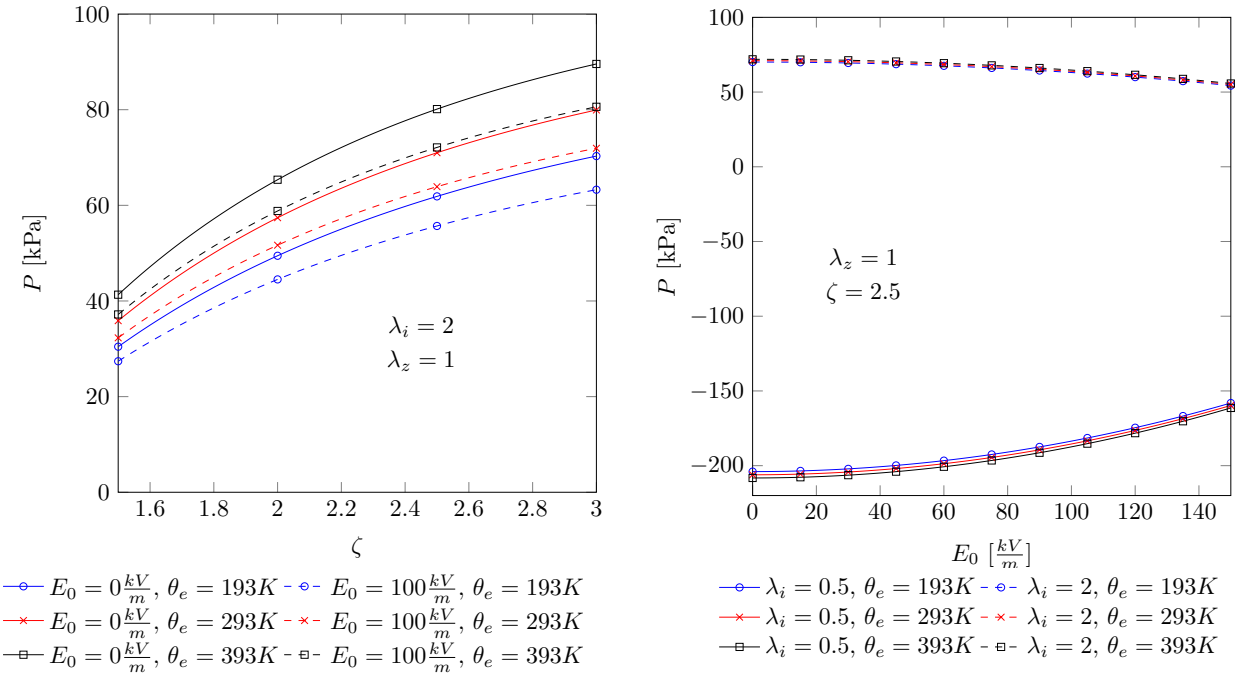

Figure 4: Variation of the pressure under a thermo-electro-mechanically coupled load for selected values of ζ and E_0

of the tube ($\lambda_i > 1$) at a constant volume leads to a contraction in the axial direction for a prescribed value of $\lambda_z = 1$, there has to be a positive normal force acting in the axial direction to prevent any contraction. For an increased tube thickness the level of the normal force increases as well. This behavior is plotted in Fig (5a). The applied electric field instigates the material to contract in the axial direction. Simultaneously, the electric field leads to a softening of the material due to the dependency of the shear modulus on I_4. As the softening effect has a stronger influence than the instigated contraction, the applied load $\bar{\mathcal{N}}$ decreases in both cases. Fig (5b) shows the response of the normal force $\bar{\mathcal{N}}$ with respect to the axial stretch λ_z. For increased values of the axial stretch characterized by λ_z, the normalized force $\bar{\mathcal{N}}$ has to increase and as before the magnitude of the normal force decreases if an electric field is applied. It is visible for the normal force as well as for the pressure that the influence of the electric field on the material response is stronger for larger values of the tube thickness.

At this stage, we take into account a radial temperature gradient for the case of normal force variation. As before this is achieved by a temperature change at the external surface of the tube while the temperature at the internal tube surface is kept constant at the reference temperature θ_0. A plot of this case shows that the normal force needed to maintain the axial stretch increases if the temperature at the external surface is increased. In contrast, the cooling of the external surface leads to a decrease in the normal force. This effect strongly depends also on the thickness of the tube, cf. Fig (6).

For increasing values of λ_i and λ_z the relative influence of the temperature gradient slightly decreases. In Fig (7) the normal force is plotted with respect to ζ and the electric field strength E_0.

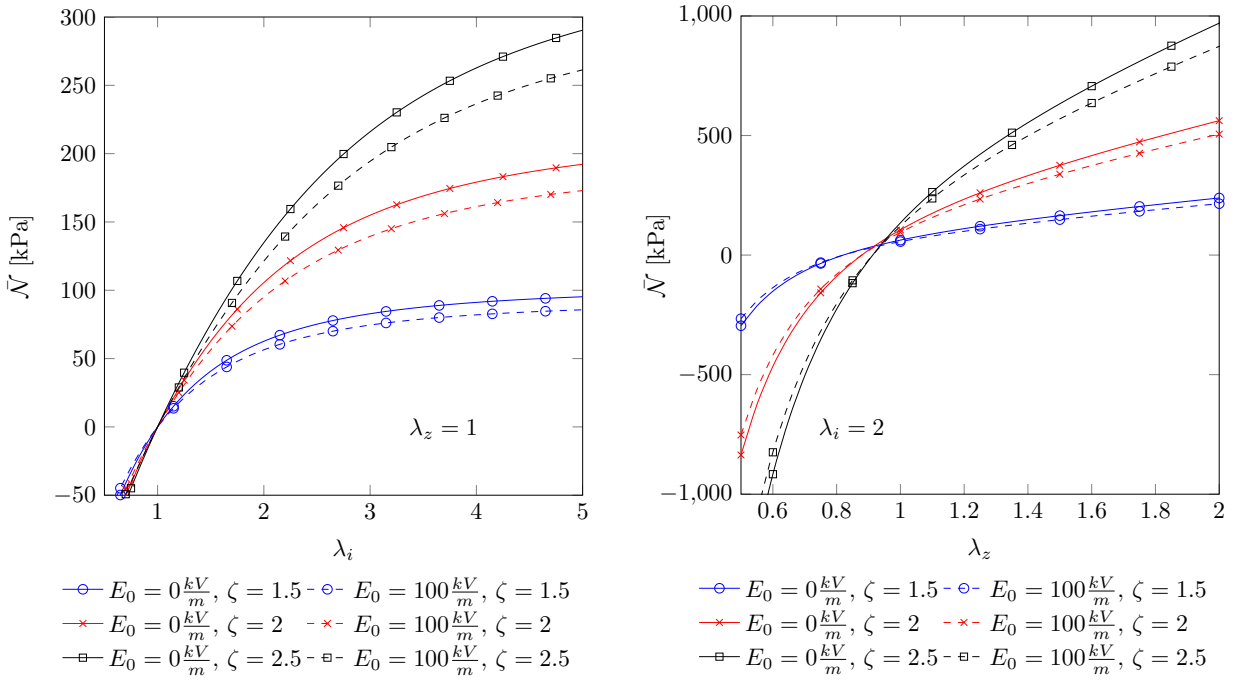

Figure 5: Plot of the normal force in the electro-mechanical case for selected values of λ_i and λ_z

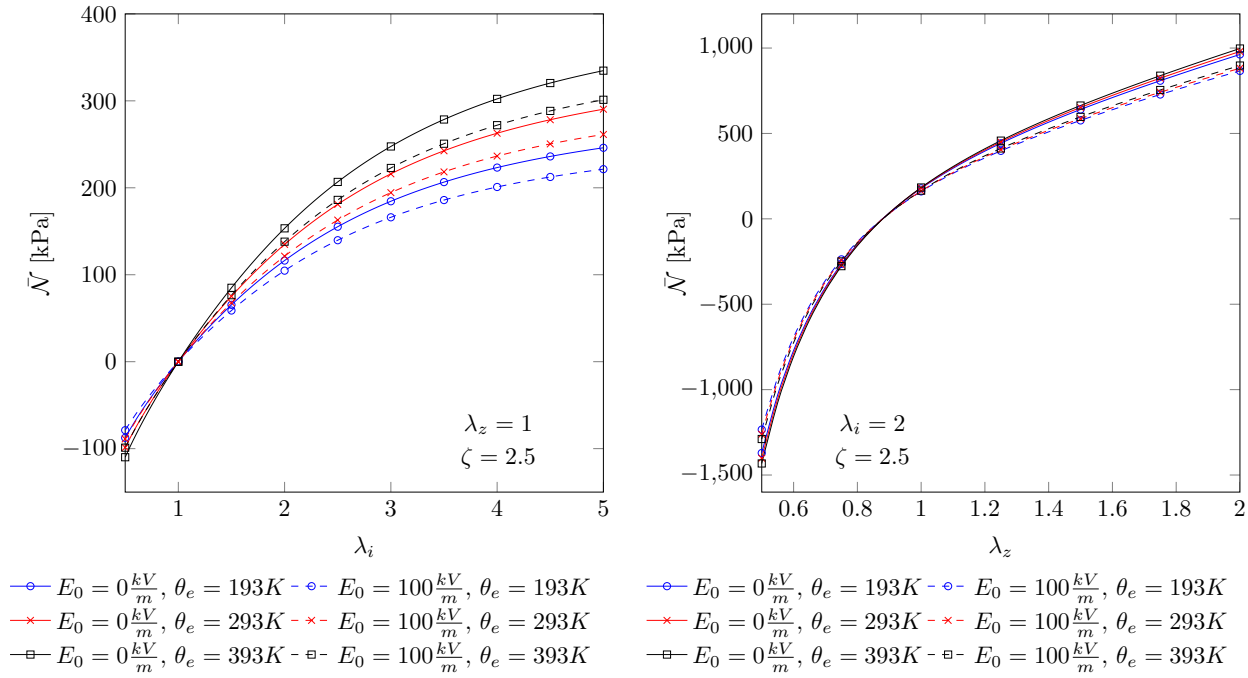

Figure 6: Plot of the normal force in the thermo-electro-mechanical case for selected values of λ_i and λ_z

Fig (7) shows that the difference between the values for the isothermal case and the cases with temperature

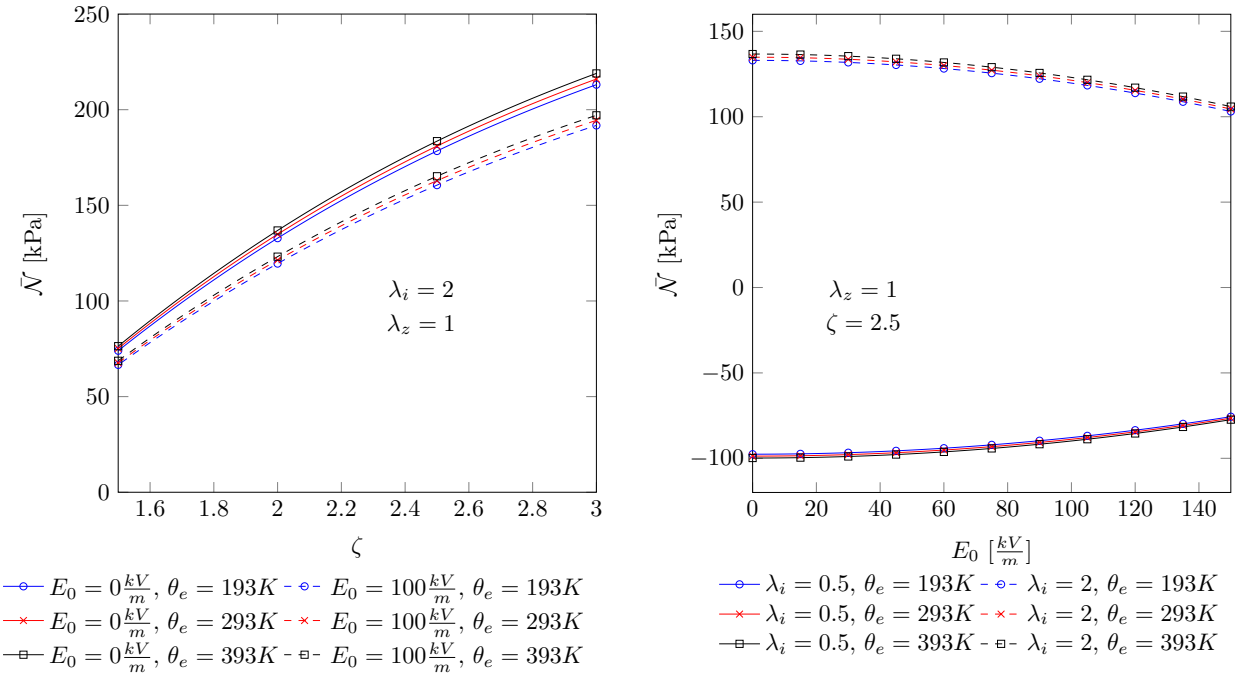

Figure 7: Plot of the normal force in the thermo-electro-mechanical case for selected values of ζ and E_0

gradient increases. Similar to the previously presented behavior of the pressure, it can be shown that the ratio of the normal force in both cases decreases which means a decreased influence of the temperature due to a smaller temperature gradient. Furthermore the right plot in Fig (7) confirms that a temperature gradient has only little influence on the normal force in the case of compression but a stronger influence in the case of tube inflation.

Finally we focus solely on the thermal behavior of the material. Therefore, both the absolute pressure and the pressure ratio with respect to the pressure at the reference temperature are plotted in Fig (8) depending on the temperature at the external tube surface. The temperature at the internal surface is kept constant and is equal to the reference temperature $\theta_0 = 293K$. We vary the value of λ_i to evaluate radial compression ($\lambda_i < 1$), inflation ($\lambda_i > 1$) and a case without the mechanical deformation ($\lambda_i = 1$)

In the case of compression, the absolute influence of the temperature change on the pressure is more distinctive compared to the case of inflation but the relative change is smaller due to the increased tube thickness in the case of compression, cf. Fig (8). Now we vary the value of the axial stretch λ_z, cf. Fig (9). We evaluate the cases of axial compression ($\lambda_z < 1$), elongation ($\lambda_z > 1$) and again without mechanical deformation ($\lambda_z = 1$).

Again the absolute influence of a temperature gradient on the pressure is the strongest for the largest thickness of the tube, i.e. for the smallest values of λ_z but here the change in the pressure ratio is not as distinctive as in the previous example due to the smaller influence of λ_z on the wall thickness of the tube. Finally the

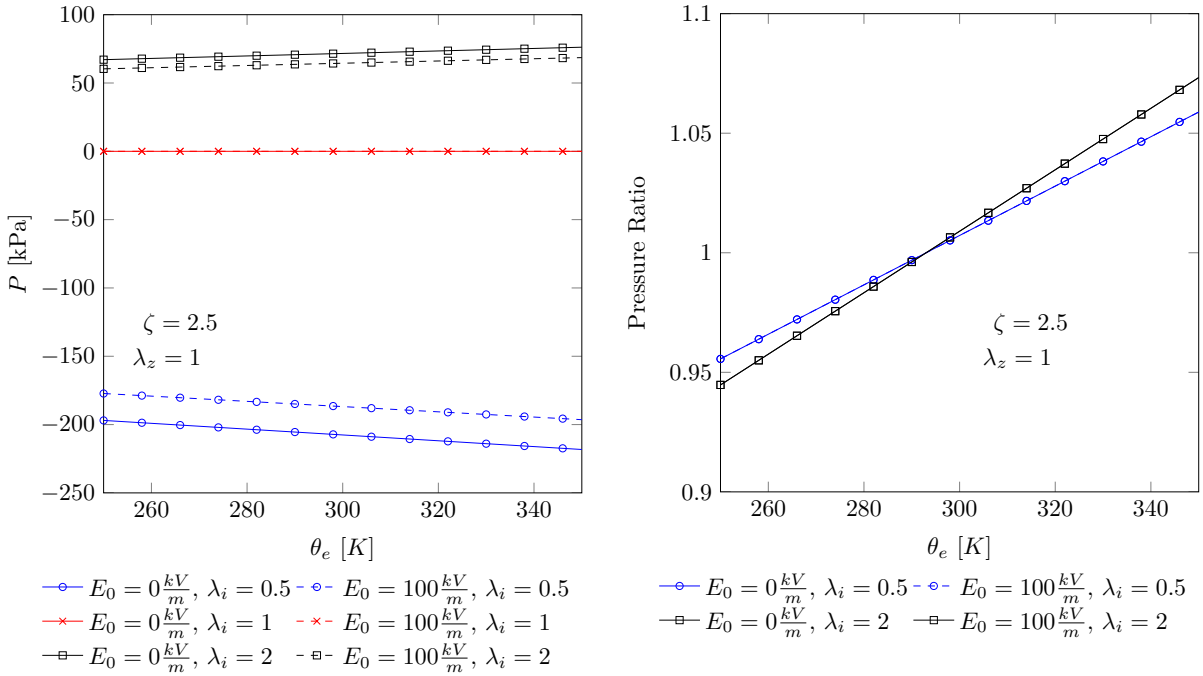

Figure 8: Plot of the pressure in the thermo-electro-mechanical case for selected values of the external temperature θ_e

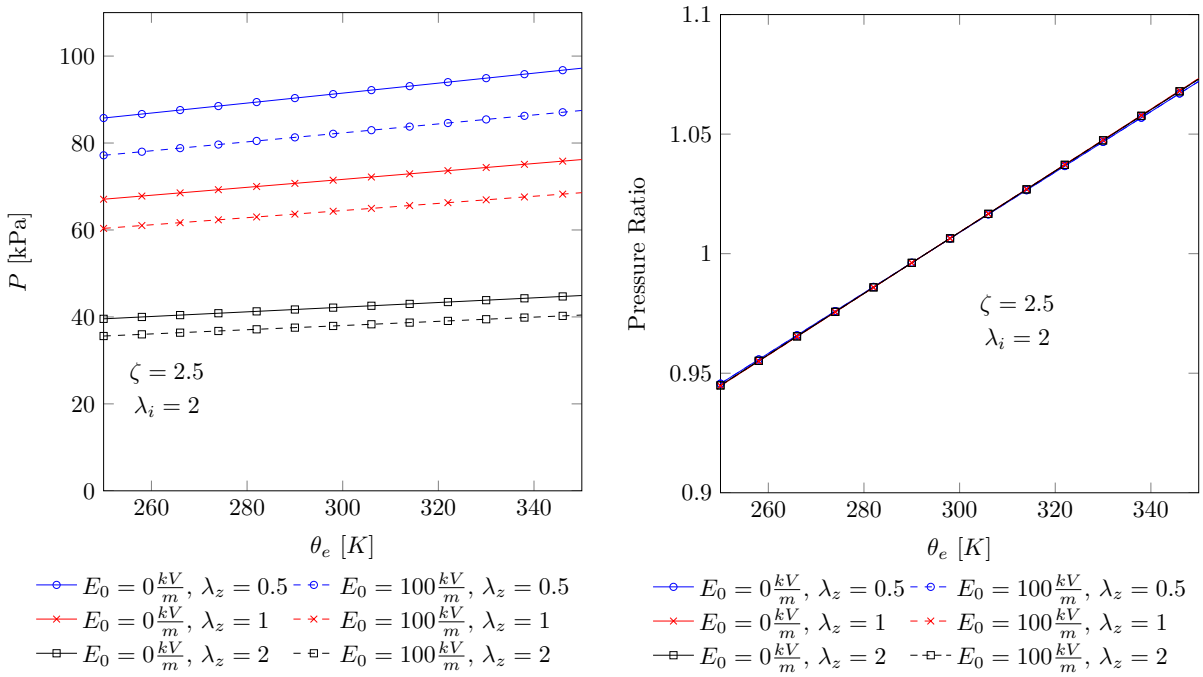

Figure 9: Plot of the pressure in the thermo-electro-mechanical case for selected values of the external temperature θ_e

influence of the initial tube thickness is analyzed, cf. Fig (10). The tube has to remain thick-walled ($\zeta > 1$) as for the thin-walled case the temperature function is not defined.

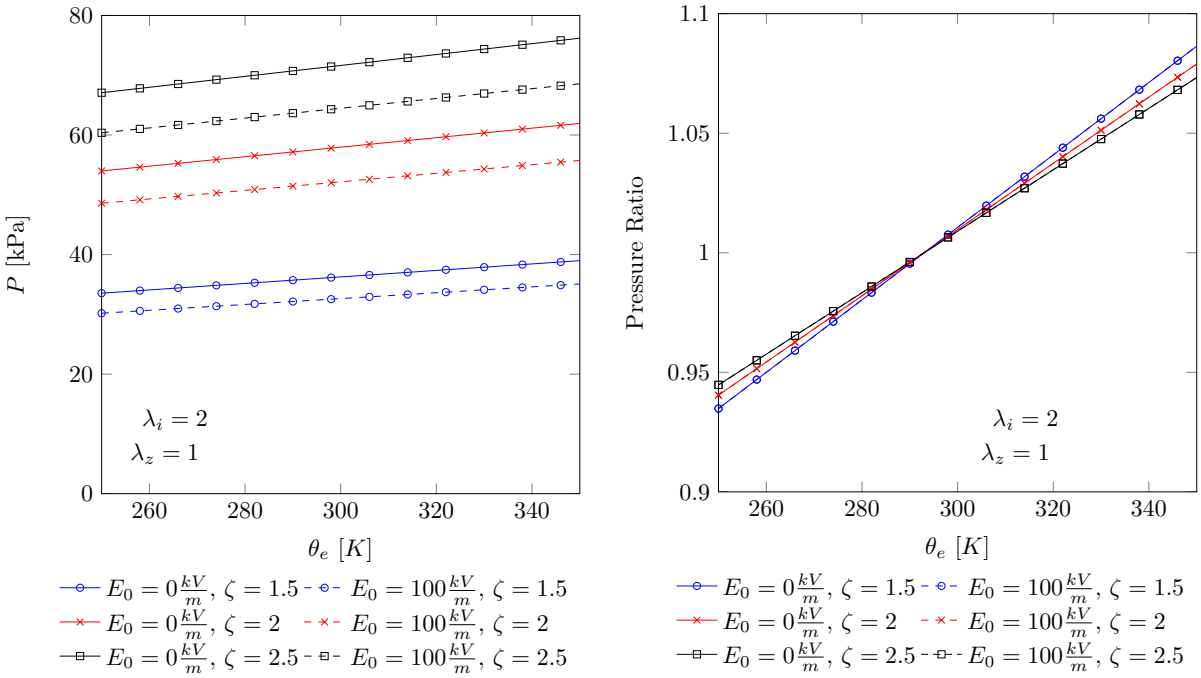

Figure 10: Plot of the pressure in the thermo-electro-mechanical case for selected values of the external temperature θ_e

In this case the ratio of the pressure shows clearly that a temperature change has the strongest influence on the pressure for the smallest tube thickness as this leads to a larger temperature gradient, cf. Fig (10).

5. Conclusion and outlook

Experimental studies of electro-active polymers under isothermal conditions are rather difficult to perform. Moreover, constraining temperature variation during tests is far from reality since polymeric materials are prone to temperature generation during experimental studies. Therefore, the formulation of a thermo-electro-mechanically coupled modelling framework is necessary to capture realistic experimental results. In this contribution, we propose a thermo-electro-mechanically coupled constitutive framework that obeys relevant laws of thermodynamics. To make the model plausible, a widely used non-homogeneous boundary value problem, i.e. a cylindrical tube subject to an electro-mechanical load in addition to a thermal load is performed. As a first step towards a comprehensive thermo-electro-mechanical approach, the time-dependence, e.g. inelasticity of the underlying polymeric materials is discarded. Therefore, the proposed model needs to be extended for viscoelastic dissipative behavior. Moreover in order to find an analytical solution several simplifications are made. For example a constant heat coefficient $c_{\boldsymbol{F},\mathbb{E}}$ and a linear Fourier law with a constant thermal conductive coefficient κ are assumed. The implementation of more general forms of these terms needs to be addressed in future contributions. In order to simulate real life boundary value problems and complex geometries, the framework needs to be implemented into a coupled finite element framework. In a forthcoming contribution, a detailed finite element implementation of the thermo-electro-mechanically coupled formulations will be elaborated. In the future, there are plans to conduct some experimental studies in order to identify constitutive material parameters and to validate the model with real

experimental data.

Data accessibility statement:

This work does not have any experimental data

Ethics statement:

This work did not contain any collection of human data

Competing interests statement:

We have no competing interests

Authors' contributions:

MM and MH jointly wrote the initial draft of the paper while MM performed the numerical calculations in the result section. PS improved the initial draft significantly. All authors gave final approval for publication.

Acknowledgements:

The authors acknowledge the funding within the DFG project No. STE 544/52-1. The second and third authors would like to express their sincere gratitude to the funding by the ERC within the Advanced Grant project MOCOPOLY.

6. Appendix

6.1. Derivation of pressure P

$$P = 2\int_{a_i}^{a_e} \frac{1}{r}\Big[\Big[\lambda^2 - \lambda^{-2}\lambda_z^{-2}\Big]\Omega_1 + \Big[\lambda^2\lambda_z^2 - \lambda^{-2}\Big]\Omega_2\Big]\mathrm{d}r \tag{77}$$

with $\Omega_1 = \frac{\theta(r)}{2\theta_0}[g_0 + g_1 I_4]$, $\Omega_2 = 0$, $\lambda = \frac{r}{R}$, $R^2 = \lambda_z[r^2 - a_i^2] + A_i^2$, $\lambda_i = \frac{a_i}{A_i}, \lambda_e = \frac{a_e}{A_e}$ it follows that:

$$\begin{aligned} P = &\underbrace{\frac{[g_0 + g_1 I_4]k_1}{\theta_0}\int_{a_i}^{a_e} \frac{r}{\lambda_z[r^2 - a_i^2] + A_i^2} - \frac{\lambda_z[r^2 - a_i^2] + A_i^2}{r^3\lambda_z^2}\mathrm{d}r}_{P_1} \\ &+ \underbrace{\frac{[g_0 + g_1 I_4]k_2}{\theta_0}\int_{a_i}^{a_e} \frac{r\ln(r)}{\lambda_z[r^2 - a_i^2] + A_i^2} - \frac{\Big[\lambda_z[r^2 - a_i^2] + A_i^2\Big]\ln(r)}{r^3\lambda_z^2}\mathrm{d}r}_{P_2} \end{aligned} \tag{78}$$

The two parts of the pressure P_1 and P_2 are evaluated separately. With $\lambda_i^2\lambda_z - 1 = \Big[\lambda_e^2\lambda_z - 1\Big]\frac{A_e^2}{A_i^2}$ we find

for P_1

$$P_1 = \frac{[g_0 + g_1 I_4]k_1}{\theta_0}\Big[\frac{1}{\lambda_z}\ln\Big(\frac{\lambda_i}{\lambda_e}\Big) - \frac{1}{2\lambda_z^2}\Big[\frac{1}{\lambda_i^2} - \frac{1}{\lambda_e^2}\Big]\Big] \tag{79}$$

In the same fashion the term P_2 can be transformed

$$\begin{aligned} P_2 = &\frac{[g_0 + g_1 I_4]k_2}{\theta_0}\int_{a_i}^{a_e}\frac{r\ln(r)}{\lambda_z[r^2 - a_i^2] + A_i^2}\mathrm{d}r \\ &- \frac{[g_0 + g_1 I_4]k_2}{\theta_0}\left[\frac{1}{2\lambda_z}\Big[\ln^2(a_e) - \ln^2(a_i)\Big] - \frac{\Big(A_i^2 - \lambda_z a_i^2\Big)}{\lambda_z^2}\Big[\frac{\ln(a_e)}{2a_e^2} - \frac{\ln(a_i)}{2a_i^2} + \frac{1}{4}\Big[a_e^{-2} - a_i^{-2}\Big]\Big]\right] \end{aligned} \tag{80}$$

The remaining integral is evaluated with Maple 18.

6.2. Derivation of axial Force N

With the axial component of the mechanical tractions at the end of the tube we obtain:

$$N = 2\pi\int_{a_i}^{a_e} t_z r\mathrm{d}r = 2\pi\int_{a_i}^{a_e}[\sigma_{zz} - \sigma_{zz}^{\max}]r\mathrm{d}r. \tag{81}$$

First we focus on the part of the integral that contains the Maxwell stress

$$-2\pi\int_{a_i}^{a_e}\sigma_{zz}^{\max}r\mathrm{d}r = -2\pi\int_{a_i}^{a_e}\frac{1}{2}\varepsilon_0\lambda_z^{-2}E_0^2 r\mathrm{d}r \quad = -\frac{1}{2}\pi\varepsilon_0\lambda_z^{-2}E_0^2[a_e^2 - a_i^2]. \tag{82}$$

Finally we concentrate on the total Cauchy stress

$$\begin{aligned} &2\pi\int_{a_i}^{a_e}\sigma_{zz}^{\mathrm{tot}}r\mathrm{d}r = 2\pi\int_{a_i}^{a_e}[-p + 2\lambda_z^2\Omega_1 - 2E_0^2\lambda_z^{-2}\Omega_5]r\mathrm{d}r \\ &= \underbrace{2\pi\int_{a_i}^{a_e}[\frac{1}{2}[\sigma_{rr}^{\mathrm{tot}} + \sigma_{\phi\phi}^{\mathrm{tot}}]r\mathrm{d}r}_{\mathcal{N}_1} + \underbrace{2\pi\int_{a_i}^{a_e}[2\lambda_z^2 - \lambda_z^{-2}\lambda^{-2} - \lambda^2]\Omega_1 r\mathrm{d}r}_{\mathcal{N}_2} - \underbrace{2\pi\int_{a_i}^{a_e}2E_0^2\lambda_z^{-2}\Omega_5 r\mathrm{d}r}_{\mathcal{N}_3} \end{aligned} \tag{83}$$

with $\Omega_5 = \frac{\theta(r)}{\theta_0}c_2 = \frac{\theta(r)}{\theta_0}\frac{\epsilon_0}{2}$. The terms $\mathcal{N}_1$, $\mathcal{N}_2$ and $\mathcal{N}_3$ are evaluated separately as

$$\mathcal{N}_1 = 2\pi\int_{a_i}^{a_e}[\frac{1}{2}[\sigma_{rr}^{\mathrm{tot}} + \sigma_{\phi\phi}^{\mathrm{tot}}]r\mathrm{d}r = \pi\left[[\sigma_{rr}^{\mathrm{tot}}(r)\frac{r^2}{2}]_{a_i}^{a_e} - \int_{a_i}^{a_e}\frac{\partial\sigma_{rr}^{\mathrm{tot}}}{\partial r}\frac{r^2}{2}\mathrm{d}r + \int_{a_i}^{a_e}\sigma_{\phi\phi}^{\mathrm{tot}}r\mathrm{d}r\right] \tag{84}$$

with $\frac{\partial\sigma_{rr}^{\mathrm{tot}}}{\partial r}r = \sigma_{\phi\phi}^{\mathrm{tot}} - \sigma_{rr}^{\mathrm{tot}}$ we find

$$= \pi\left[\frac{1}{2}[\sigma_{rr}^{\max}]a_e^2 - \frac{1}{2}[\sigma_{rr}^{\max} - P]a_i^2 + \int_{a_i}^{a_e}[\sigma_{\phi\phi}^{\mathrm{tot}} + \sigma_{rr}^{\mathrm{tot}}]\frac{r}{2}\mathrm{d}r\right]. \tag{85}$$

The last term is identical to the initial integral. Thus it is subtracted to the left side of the equation which leads to

$$\mathcal{N}_1 = -\frac{1}{2}\pi\varepsilon_0\lambda_z^{-2}E_0^2[a_e^2 - a_i^2] + \pi P a_i^2 \tag{86}$$

For $\mathcal{N}_2$ we obtain

$$\begin{aligned}\mathcal{N}_2 = &\frac{2\pi\Omega_1 k_1}{\theta_0}\int_{a_i}^{a_e} 2\lambda_z^2 r - \frac{(r^2-a_i^2)\lambda_z + A_i^2}{r\lambda_z^2} - \frac{r^3}{(r^2-a_i^2)\lambda_z + A_i^2}\mathrm{d}r \\ &+ \frac{2\pi\Omega_1 k_2}{\theta_0}\int_{a_i}^{a_e} 2\lambda_z^2 r\ln(r) - \frac{(r^2-a_i^2)\lambda_z + A_i^2}{r\lambda_z^2}\ln(r) - \frac{r^3\ln(r)}{(r^2-a_i^2)\lambda_z + A_i^2}\mathrm{d}r\end{aligned} \tag{87}$$

which is simplified as

$$\begin{aligned}\mathcal{N}_2 = &\frac{2\pi\Omega_1 k_1}{\theta_0}\left[[\lambda_z^2 - \frac{1}{\lambda_z}][a_e^2 - a_i^2] + \frac{A_i^2 - a_i^2\lambda_z}{\lambda_z^2}\ln(\frac{\lambda_i}{\lambda_e})\right] \\ &+ \frac{2\pi\Omega_1 k_2}{\theta_0}\left[[2\lambda_z^2 - \frac{1}{\lambda_z}][-\frac{1}{4}[a_e^2 - a_i^2] + \frac{1}{2}[a_e^2\ln(a_e) - a_i^2\ln(a_i)]]\right] \\ &- \frac{2\pi\Omega_1 k_2}{\theta_0}\left[\frac{A_i^2 - a_i^2\lambda_z}{2\lambda_z^2}[\ln^2(a_e) - \ln^2(a_i)]\right] - \frac{2\pi\Omega_1 k_2}{\theta_0}\int_{a_i}^{a_e}\frac{r^3\ln(r)}{(r^2-a_i^2)\lambda_z + A_i^2}\mathrm{d}r\end{aligned} \tag{88}$$

Finally we look at the third part $\mathcal{N}_3$

$$\begin{aligned}\mathcal{N}_3 &= -2\pi\int_{a_i}^{a_e} 2E_0^2\lambda_z^{-2}\Omega_5 r\mathrm{d}r = -2\pi\int_{a_i}^{a_e} 2E_0^2\lambda_z^{-2}\frac{\theta(r)}{\theta_0}\frac{\varepsilon_0}{2}r\mathrm{d}r \\ &= -\frac{2\pi E_0^2\lambda_z^{-2}\varepsilon_0}{\theta_0}\big[\frac{k_1}{2}[a_e^2 - a_i^2] + k_2[-\frac{1}{4}[a_e^2 - a_i^2] + \frac{1}{2}[a_e^2\ln(a_e) - a_i^2\ln(a_i)]]\big].\end{aligned} \tag{89}$$

When we put all of the terms together we end up with the following expression

$$\begin{aligned}\mathcal{N} = &-\frac{1}{2}\pi\varepsilon_0\lambda_z^{-2}E_0^2[a_e^2 - a_i^2] + \pi P a_i^2 \\ &+ \frac{2\pi\Omega_1 k_1}{\theta_0}\left[[\lambda_z^2 - \frac{1}{\lambda_z}][a_e^2 - a_i^2] + \frac{A_i^2 - a_i^2\lambda_z}{\lambda_z^2}\ln(\frac{\lambda_i}{\lambda_e})\right] \\ &+ \frac{2\pi\Omega_1 k_2}{\theta_0}\left[[2\lambda_z^2 - \frac{1}{\lambda_z}][-\frac{1}{4}[a_e^2 - a_i^2] + \frac{1}{2}[a_e^2\ln(a_e) - a_i^2\ln(a_i)]\right] \\ &- \frac{2\pi\Omega_1 k_2}{\theta_0}\left[\frac{A_i^2 - a_i^2\lambda_z}{2\lambda_z^2}[\ln^2(a_e) - \ln^2(a_i)]\right] - \frac{2\pi\Omega_1 k_2}{\theta_0}\int_{a_i}^{a_e}\frac{r^3\ln(r)}{[r^2 - a_i^2]\lambda_z + A_i^2}\mathrm{d}r \\ &-\frac{2\pi E_0^2\lambda_z^{-2}\varepsilon_0}{\theta_0}\big[\frac{k_1}{2}[a_e^2 - a_i^2] + k_2[-\frac{1}{4}[a_e^2 - a_i^2] + \frac{1}{2}[a_e^2\ln(a_e) - a_i^2\ln(a_i)]]\big] \\ &- \frac{1}{2}\pi\varepsilon_0\lambda_z^{-2}E_0^2[a_e^2 - a_i^2].\end{aligned} \tag{90}$$

Further manipulation and integration of the formulation for the pressure leads to the final formulation

$$
\begin{aligned}
\mathcal{N} =& \pi\varepsilon_0 E_0^2[-\frac{k_1\lambda_z^{-2}}{\theta_0} - \lambda_z^{-2}][a_e^2 - a_i^2] + \frac{2\Omega_1 k_2 \pi}{\theta_0}\int_{a_i}^{a_e} \frac{[a_i^2 r - r^3]\ln(r)}{\lambda_z[r^2 - a_i^2] + A_i^2}\mathrm{d}r \\
&+ \frac{2\Omega_1 k_2 a_i^2 \pi}{\theta_0}\left[\frac{(A_i^2 - \lambda_z a_i^2)}{\lambda_z^2}[\frac{\ln(a_e)}{2a_e^2} - \frac{\ln(a_i)}{2a_i^2} + \frac{1}{4}[a_e^{-2} - a_i^{-2}]]\right] \\
&+ \frac{2\pi\Omega_1 k_1}{\theta_0}\left[[\lambda_z^2 - \frac{1}{\lambda_z}][a_e^2 - a_i^2] - \frac{a_i^2}{2\lambda_z^2}[\frac{1}{\lambda_i^2} - \frac{1}{\lambda_e^2}] + \frac{A_i^2}{\lambda_z^2}\ln(\frac{\lambda_i}{\lambda_e})\right] \\
&+ \frac{2\pi\Omega_1 k_2}{\theta_0}\left[[2\lambda_z^2 - \frac{1}{\lambda_z}][-\frac{1}{4}[a_e^2 - a_i^2] + \frac{1}{2}[a_e^2\ln(a_e) - a_i^2\ln(a_i)] - \frac{A_i^2}{2\lambda_z^2}[\ln^2(a_e) - \ln^2(a_i)]\right] \\
&- \frac{2\pi E_0^2\lambda_z^{-2}\varepsilon_0}{\theta_0}\left[k_2[-\frac{1}{4}[a_e^2 - a_i^2] + \frac{1}{2}[a_e^2\ln(a_e) - a_i^2\ln(a_i)]]\right].
\end{aligned}
\tag{91}
$$

References:

[1] F. Vogel, *On the modeling and computation of electro- and magneto-active polymers*, Dissertation, Friedrich-Alexander-University Erlangen-Nuremberg, Germany, 2014.

[2] F. Vogel, S. Goektepe, E. Kuhl, P. Steinmann, *Modeling and simulation of viscous electro-active polymers*, European Journal of Mechanics A/Solids, 48:112-128, 2014

[3] P. Steinmann, *Computational nonlinear electro-elasticity-getting started*, CISM International Centre for Mechanical Sciences, Vol. 527, 2011.

[4] R. Vertechy, G. Berselli, V. P. Castelli, M. Bergamasco, *Continuum thermo-electro-mechanical model for electrostrictive elastomers*, Journal of Intelligent Material Systems and Structures, 24:761-778, 2012

[5] R. Vertechy, G. Berselli, V. P. Castelli, G. Vassura, *Optimal design of Lozenge-shaped dielectric elastomer linear actuators: Mathematical procedure and experimental validation*, Journal of Intelligent Material Systems and Structures, 21:503-515, 2010

[6] R. Vertechy, M. Fontana, G. R. Papini, D. Forehand, *In-tank tests of a dielectric elastomer generator for wave energy harvesting*, In SPIE Smart Structures and Materials- Nondestructive Evaluation and Health Monitoring, 90561G-90561G, International Society for Optics and Photonics, 2014

[7] R. Vertechy, M. Fontana, *Electromechanical characterization of a new synthetic rubber membrane for dielectric elastomer transducers*, In Proc. SPIE 9430, Electroactive Polymer Actuators and Devices (EAPAD), 90561F, DOI: 10.1117/12.2045086, San Diego (CA), 8-12 March 2015.

[8] R. Kaltseis, C. Keplinger, S. J. A. Koh, R. Baumgartner, Y. F. Goh, W. H. Ng, A. Kogler, A. Troels, C. C. Foo, Z. Suo and S. Bauer, *Natural rubber for sustainable high-power electrical energy generation*, RSC Advances, 4, 27905, 2014.

[9] H. Boese, Holger, E. Fuss, *Novel dielectric elastomer sensors for compression load detection*, SPIE Smart Structures and Materials- Nondestructive Evaluation and Health Monitoring, International Society for Optics and Photonics, 2014.

[10] S. J. A. Koh, C. Keplinger, T. Li, S. Bauer, Z. Suo, *Dielectric elastomer generators: How much energy can be converted?*, Mechatronics, IEEE/ASME Transactions , 33-41, 16(1), 2011.

[11] P. Chadwick, *Thermo-mechanics of rubberlike materials*, Philosophical Transactions of the Royal Society of London. Series A, Mathematical and Physical Sciences, 276:371-403, 1974

[12] G. A. Holzapfel, J. C. Simo, *Entropy elasticity of isotropic rubber-like solids at finite strains*, Computer Methods in Appied Mechanics and Engineering, 132:17-44,1996

[13] D. K. Vu, P. Steinmann, *Numerical modeling of non-Linear electroelasticity*, International Journal for Numerical Methods in Engineering, 70:685-704, 2007

[14] P. Monk, *Finite Element Methods for Maxwell Equations*, Oxford University Press, Clarendon (2003)

[15] R. Bustamante, *Transversely isotropic nonlinear magneto-active elastomers*, Acta Mechanica, 210(3-4):183-214, 2010

[16] R. Bustamante, *Transversely isotropic nonlinear electro-active elastomers*, Acta Mechanica, 206(3-4):237-259, 2009

[17] R. Bustamante, *A variational formulation for a boundary value problem considering an electro-sensitive elastomer interacting with two bodies*, Mechanics Research Communication 36 (7):791-795, 2009

[18] D. R. Bland, *Elastoplastic thick-walled tubes of work-hardening material subject to internal and external pressures and to temperature gradients*, Journal of the Mechanics and Physics of Solids, 4:209-229, 1956

[19] K. R. Rajagopal, Y. N. Huang, *Finite circumferential shearing of nonlinear solids in the context of thermoelasticity*, Journal of Applied Mathematics, 53:111-125, 1994

[20] A. Ask, A. Menzel, M. Ristinma, *Phenomenological modeling of viscous electrostrictive polymers*, International Journal of Non-Linear Mechanics, 47(2):156-165, 2012

[21] A. Ask, A. Menzel, M. Ristinma, *Electrostriction in electro-viscoelastic polymers*, Mechanics of Materials, 50:9-21,2012

[22] A. Büschel, S. Klinkel, W. Wagner, *Dielectric elastomers-Numerical modeling of nonlinear viscoelasticity*, International Journal of Numerical Methods in Engineering, 93:834-856, 2013

[23] E. Arruda, M. C. Boyce, *A three-dimensional constitutive model for the large stretch behavior of rubber elastic materials*, Journal of the Mechanics and Physics of Solids, 41:389-412,1993

[24] J. S. Bergström, M. C. Boyce, *Constitutive modeling of the large strain time-dependent behavior of elastomers*, Journal of the Mechanics and Physics of Solids, 46:931-954, 1998

[25] P. Saxena, M. Hossain, P. Steinmann *A theory of finite deformation magneto-viscoelasticity*, International Journal of Solids and Structures, 50(24):3886-3897, 2013

[26] P. Saxena, D. K. Vu, P. Steinmann *On rate-dependent dissipation effects in electro-elasticity*, International Journal of Non-Linear Mechanics, 62:1-11, 2014

[27] B. D. Coleman, M. E. Gurtin, *Thermodynamics with internal state variables*, Journal of Chemical Physics, 47:597-613, 1967

[28] M. Johlitz, H. Steeb, S. Diebels, A. Chatzouridou, J. Batal, W. Possart, *Experimental and theoretical investigation of nonlinear viscoelastic polyurethane systems*, Journal of Materials Science, 42:9894-9904, 2007

[29] S. Reese, S. Govindjee, *A theory of finite viscoelasticity and numerical aspects*, International Journal of Solids and Structures, 35:3455-3482, 1998

[30] D. K. Vu, P. Steinmann, *A 2-D coupled BEM-FEM simulation of electro-elastostatics at large strain*, Computer Methods in Applied Mechanics and Engineering, 199:1124-1133, 2010

[31] I. Diaconu, D. O. Dorohoi, C. Ciobanu, *Electromechanical response of polyurethane films with different thickness*, Romanian Journal of Physics, 53(1-2):91-97, 2008

[32] R. M. McMeeking, C. M. Landis, *Electrostatic forces and stored energy for deformable dielectric materials*, Journal of Applied Mechanics, 72:581-590, 2005

[33] W. Ma, L. E. Cross, *An experimental investigation of electromechanical response in a dieletric acrylic elastomer*, Applied Physics A, 78:1201-1204, 2004

[34] S. Michel, X. Q. Zhang, M. Wissler, C. Löwe, G. Kovocs, *A comparison between silicone and acrylic elastomers as dielectric materials in electroactive polymer actuators*, Polymer International, 59:391-399,2010

[35] J. Qiang, H. Chen and B. Li, *Experimental study on the dielectric properties of polyacrylate dielectric elastomer*, Smart Material Structures, 21:1-9, 2012

[36] P. Steinmann, M. Hossain, G. Possart, *Hyperelastic models for rubber-like materials: Consistent tangent operators and suitability of Treloar's data*, Archive of Applied Mechanics, 82(9):1183-1217, 2012

[37] M. Wissler, E. Mazza, *Mechanical behavior of an acrylic elastomer used in dielectric elastomer actuators*, Sensors and Actuators A, 134:494-504, 2007

[38] Z. Gao, A. Tuncer, A. H. Cuitino, *Modeling and simulation of the coupled mechanical-electrical response of soft solids*, International Journal of Plasticity, 27(10):1459-1470, 2011

[39] A. Dorfmann, R. W. Ogden, *Nonlinear electroelasticity*, Acta Mechanica, 174(3):167-183, 2005

[40] A. Dorfmann, R. W. Ogden, *Nonlinear electroelastic deformations*, Journal of Elasticity, 82(2):99-127, 2006

[41] Y. Bar-Cohen, *Electro-active polymers: current capabilities and challenges*, *EAPAD Conference, San Diego, CA, March 18-21* 2002; 4695–02.

[42] A. Dorfmann, R. W. Ogden, *Magnetoelastic modelling of elastomers*, European Journal of Mechanics A/Solids, 22(4):497-507, 2003

[43] A. Dorfmann, R. W. Ogden, *Nonlinear magnetoelastic deformations of elastomers*, Acta Mechanica, 167(1-2):13-28, 2004

[44] A. Dorfmann, R. W. Ogden, *Nonlinear magnetoelastic deformations*, Quarterly Journal of Mechanics and Applied Mathematics, 57(4):599-622, 2004

[45] A. Dorfmann, R. W. Ogden, *Some problems in nonlinear magnetoelasticity*, ZAMP, 56(4):718-745, 2005

[46] A. Dorfmann, I. A. Brigdanov, *Constitutive modelling of magneto-sensitive Cauchy elastic solids*, Computational Materials Science, 29(3):270-282, 2004

[47] I. A. Brigdanov, A. Dorfmann, *Mathematical modeling of magneto-sensitive elastomers*, *International Journal of Solids and Structures*, 40(18):4659-4674, 2003

[48] G. A. Maugin, *Continuum mechanics of electromagnetic solids*, North-Holland (1988)

[49] P. A. Voltairas, D. I. Fotiadis, C. V. Massalas, *A theoretical study of the hyperelasticity of electro-gels*, Proceedings of the Royal Society A, 459:2121-2130, 2003

[50] D. J. Griffiths, *Introduction to Electrodynamics, 3rd ed.* Prentice Hall (1998)

[51] A. Kovetz, *Electromagnetic theory*. Oxford University Press (2000)

[52] Y. H. Pao, *Electromagnetic forces in deformable continua*, Mechanics Today, (Nemat- Nasser, S., ed.), Oxford: Pergamon Press. 1978; **4**:209-306.

[53] R. W. Ogden RW, *Nonlinear elastic deformations*. Dover (1997)

[54] Maplesoft. *Maple 9 Learning Guide*. Maplesoft, Waterloo Maple Inc. (2003)

[55] A. Lion, *On the large deformation behavior of reinforced rubber at different temperatures*, Journal of the Mechanics and Physics of Solids, 45:1805-1834, 1997

[56] X. Chen, *On magneto-thermo-viscoelastic deformation and fracture*, International Journal of Non-Linear Mechanics, 44:244-248, 2009

[57] X. Chen, *Nonlinear electro-thermo-viscoelasticity*, Acta Mechanica, 211:49-59, 2010

[58] S. Santapuri, R. L. Lowe, S. E. Bechtel, M. J. Dapino, *Thermodynamic modeling of fully coupled finite-deformation thermo-electro-magneto-mechanical behavior for multifunctional applications*, International Journal of Engineering Science, 72:117-139, 2013

[59] S. Santapuri, *Unified continuum modeling of fully coupled thermo-electro-magneto-mechanical behavior with applications to multifunctional materials and structures*, PhD Thesis, Ohio State University, USA, 2012

[60] Q. S. Yang, Q. H. Qin, L. H. Ma, X. Z. Lu, C. Q. Cui, *A theoretical model and finite element formulation for coupled thermo-electro-chemo-mechanical media*, Mechanics of Materials, 42:148-156, 2010

[61] M. Hossain, P. Steinmann, *More hyperelastic models for rubber-like materials: Consistent tangent operators and comparative study*, Journal of the Mechanical Behaviour of Materials, 22(1-2):27-50, 2013

[62] M. Hossain, N. Kabir, A. F. M. S. Amin, *Eight-chain and full-network models and their modified versions for rubber hyperelasticity : A comparative study*, Journal of the Mechanical Behaviour of Materials, 24(1-2):11-24, 2015

[63] M. Hossain, D. K. Vu, P. Steinmann, *Experimental study and numerical modelling of VHB 4910 polymer*, Computational Materials Science, 59:65-74, 2012

[64] M. Hossain, D. K. Vu, P. Steinmann, *A comprehensive characterization of the electro-mechanically coupled properties of VHB 4910 polymer*, Archive of Applied Mechanics, 85(4):523-537, 2014

[65] P. Erbts, S. Hartmann, A. Düster, *A partitioned solution approach for electro-thermo-mechanical problems*, Archive of Applied Mechanics, 85:1075-1101, 2015

[66] D. J. Leslie, N. H. Scott, *Incompressibility at uniform temperature or entropy in isotropic thermoelasticity* , Quarterly Journal of Applied Mathematics, 51(2):191-211, 1998

[67] A. C. Eringen, G. A. Maugin, *Electrodynamics of Continua* , Springer-Verlag (1990)

[68] L.R.G. Treloar , *The Physics of Rubber Elasticity* , Oxford University Press (1975)